

DEMYSTIFYING LLM-AS-A-JUDGE: ANALYTICALLY TRACTABLE MODEL FOR INFERENCE-TIME SCALING

Indranil Halder

John A. Paulson School of Engineering And Applied Sciences, Harvard University
ihalder@g.harvard.edu

Cengiz Pehlevan

Center for Brain Science, Harvard University
 John A. Paulson School of Engineering And Applied Sciences, Harvard University
 Kempner Institute for the Study of Natural and Artificial Intelligence, Harvard University
cpehlevan@g.harvard.edu

ABSTRACT

Recent developments in large language models have shown advantages in reallocating a notable share of computational resource from training time to inference time. However, the principles behind inference time scaling are not well understood. In this paper, we introduce an analytically tractable model of inference-time scaling: Bayesian linear regression with a reward-weighted sampler, where the reward is determined from a linear model, modeling LLM-as-a-judge scenario. We study this problem in the high-dimensional regime, where the deterministic equivalents dictate a closed-form expression for the posterior predictive mean and variance. We analyze the generalization error when training data are sampled from a teacher model. We draw k inference-time samples and select via softmax at a temperature applied to a quadratic reward. When the reward is not too different from the teacher, the generalization error decreases monotonically with increasing inference time samples k . However, the specific reward that optimizes inference-time selection generally differs from the teacher. In contrast, substantial reward misspecification induces a finite optimal k beyond which more sampling can increase the generalization error. For fixed k , there exists an optimal sampling temperature. We experimentally verify these facts in large language model inference with an additional large language model as a judge. In the “best-of- k ” limit with the teacher as reward, we theoretically show that the generalization error decays as $\Theta(1/k^2)$ and determine the leading coefficient via extreme value theory. These formulas delineate domains where scaling inference-time computation is provably preferable to collecting more data. Finally, we demonstrate that when task difficulty increases, the previously mentioned advantage of inference-time compute degrades.

Code: [GitHub repository](#)

1 INTRODUCTION

Scaling training compute via larger models and more data drives dramatic gains (Hestness et al., 2017; Kaplan et al., 2020; Hoffmann et al., 2022). In parallel, across tasks, allowing models to ‘think longer’ at inference by sampling multiple candidates, re-ranking with a reward, or aggregating votes consistently improves precision and reliability (Wang et al., 2023; Zheng et al., 2023; Zhang et al., 2024; Wu et al., 2024; Snell et al., 2025). Best-of- k (choose the highest-reward sample based on the feedback of a judge large language model) and majority voting (choose the consensus among the

generated answers) have become standard inference-time tools (Brown et al., 2024; Schaeffer et al., 2025a; Chen et al., 2024a; Huang et al., 2025a) along with self-verification (Saunders et al., 2022; Weng et al., 2023).

Despite widespread adoption, key questions for inference-time computation lack crisp answers. How to optimally configure inference-time sampling to minimize generalization error under realistic compute constraints and how to allocate compute optimally between pretraining and inference time remain open questions (Wu et al., 2024). Which reward model should we use for inference? What is the appropriate inference-time sampler, e.g., temperature settings? How large should k be and when do more samples stop helping? How should we allocate a fixed compute budget between training and inference to minimize generalization error? We lack a simple, solvable model that gives us intuitions and actionable prescriptions.

To fill this gap, we propose a minimal and analytically tractable setting: Bayesian regression based on a teacher-student setting with a controlled reward and a temperature-dependent inference-time sampler, in which best-of- k appears as limit. This setup is a proxy for LLM-as-a-judge providing reward for the generated answers from a base-LLM. We theoretically study the generalization error δ as a function of the size of the training data set n , the dimension of the data d , the number of inference time samples k , the sampling temperature T and the reward parameter \mathbf{w}_R and demonstrate various optimality conditions on these parameters.

This simple model recapitulates existing findings on large language model (LLM) inference and yields novel predictions that we evaluate in this paper. It reproduces the empirical observation that unbounded increases in the number of inference-time samples do not confer additional benefit (Snell et al., 2025). Furthermore, it predicts the existence of an optimal temperature for the reward process. Further, strong rewards shift optimal temperature to a lower value. We empirically examine and confirm this prediction using Llama-3-8B-Instruct, DeepSeek-R1-Distill-Qwen-1.5B etc.

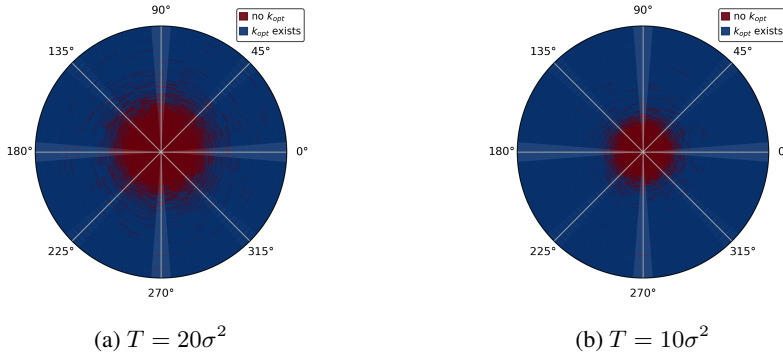


Figure 1: In the plot the radial distance c of the vector $\mathbf{w}_R - \mathbf{w}_T$ and the polar variable is the angle θ between $\mathbf{w}_R - \mathbf{w}_T$ and \mathbf{w}_T . We have chosen $S = 1, \sigma = 10^{-4}, \gamma = 10^{-3}, d = 2, n = 10^4$ and sampled teacher weight $\mathbf{w}_T = (c \cos \theta_T, c \sin \theta_T) \sim \mathcal{N}(0, 2^2 \mathbf{I})$. We have parameterized the reward weight as follows: $\mathbf{w}_R = \mathbf{w}_T + (c \cos(\theta_T + \theta), c \sin(\theta_T + \theta)), \theta \in [0, 2\pi]$. See section 2 for details of notation and conventions. From the plot, we see that as temperature T decreases the domain, where generalization error δ decreases monotonically with the increase in inference-time samples k , shrinks. Similar result is presented in remark 2 for the proportional limit.

At the technical level our contributions are the following:

- We propose a solvable model for inference-time scaling: Bayesian regression where the ground truth is given by the teacher model $y = \mathbf{w}_T \cdot \mathbf{x} / \sqrt{d}$ and the reward function is quadratic $r(y, \mathbf{x}) = -(y - \mathbf{w}_R \cdot \mathbf{x} / \sqrt{d})^2$. We generate k samples at inference and choose using a softmax at temperature T over the reward. This method is conceptually close to the importance sampling method in Faria and Smith (2025). We present a formula for the generalization error δ in the proportional limit: $d \rightarrow \infty, n \rightarrow \infty$ with $\alpha = d/n$ fixed.
- In order to derive analytic insights about the inference time optimization, we derive a series expansion for δ around large T , making explicit its dependence on n, k , and the alignment between \mathbf{w}_R and \mathbf{w}_T . The analytical expansion shows a sharp dependence on reward

quality: when \mathbf{w}_R is sufficiently close to \mathbf{w}_T , i.e., small $\|\mathbf{w}_R - \mathbf{w}_T\|/\|\mathbf{w}_T\|$, increasing k monotonically decreases δ , and the reward \mathbf{w}_R that optimizes inference-time selection generally *differs* from the data-generating teacher \mathbf{w}_T . In contrast, when \mathbf{w}_R is poorly aligned, δ is non-monotone in k , yielding an *optimal* finite k (see Figure 1), echoing phenomena observed empirically in large language models (Snell et al., 2025). Furthermore we show that at fixed k , there exists an *optimal* temperature T for the rewarding process. A similar yet distinct observation has been made in large language models (Du et al., 2025) for sampling temperature of the model itself. We emphasize that our result is about the sampling temperature of the rewarding process - different from the sampling temperature of the language model.

- To explore the best-of- k case, we consider the $T = 0$ limit. Using extreme value theory, we analytically prove that the expectation value of δ scales as $\Theta(1/k^2)$ at large k when we have access to the teacher, i.e., $\mathbf{w}_R = \mathbf{w}_T$. Based on our theoretical analysis in best-of- k limit, we quantify the parametric region where scaling inference-time compute is more *beneficial* compared to training compute. Finally we note that when task difficulty increases, the previously mentioned advantage of inference-time compute degrades.
- To test our predictions in realistic settings, we have generated inference time samples from Llama-3-8B-Instruct and DeepSeek-R1-Distill-Qwen-1.5B on openai/gsm8k validation dataset (see Appendix G.2 for the details and more empirical results). For each question and response pair we used Mistral-7B-Instruct-v0.3 or Qwen2.5-Math-PRM-7B to generate a reward score. Finally, we observed the existence of an optimal k, T similar to the theoretical predictions above (see Figure 8, 9, 10, 11 and 12). In particular for the best-of- k strategy, Figure 12 shows scaling laws similar to the one observed in theoretical analysis for a nearly ideal reward model.

Now we turn to survey the ideas in the literature related to our work.

1.1 RELATED WORKS

Method of deterministic equivalence. In the context of linear regression (Krogh and Hertz, 1992; Dicker, 2016; Dobriban and Wager, 2018; Nakkiran, 2019; Advani et al., 2020; Hastie et al., 2022), kernel regression (Sollich, 1998; Sollich and Halees, 2002; Bordelon et al., 2020; Canatar et al., 2021; Spigler et al., 2020; Simon et al., 2023; Loureiro et al., 2021), and random feature models (Hastie et al., 2022; Louart et al., 2018; Mei and Montanari, 2022; Adlam and Pennington, 2020; d’Ascoli et al., 2020; d’Ascoli et al., 2020; Loureiro et al., 2021; Bahri et al., 2022; Zavatone-Veth and Pehlevan, 2023a; Dhifallah and Lu, 2020; Hu and Lu, 2022; Maloney et al., 2022; Bach, 2024) method of deterministic equivalence (Voiculescu et al., 1992; Zee, 1996) has been used extensively for discussions of higher dimensional statistics (Misiakiewicz and Saeed, 2024; Atanasov et al., 2024). These ideas have been used to discuss training time scaling laws in simple models (Spigler et al., 2020; Bordelon et al., 2020; Bahri et al., 2022; Maloney et al., 2022; Simon et al., 2021; Bordelon et al., 2024; Zavatone-Veth and Pehlevan, 2023b; Paquette et al., 2024; Lin et al., 2024; Bordelon et al., 2025). We use this technique to simplify the posterior probability distribution of the Bayesian regression model.

Inference-time scaling. A growing body of work investigates how to allocate and exploit inference-time compute to improve predictive performance, with empirical gains reported across tasks and domains based on majority voting (Chen et al., 2024a; Snell et al., 2025; Setlur et al., 2025; Arora and Zanette, 2025; Wu et al., 2024; Liu et al., 2025; Du et al., 2025; Huang et al., 2025a) or a best-of- k strategy (Wang et al., 2023; Yao et al., 2023a; Brown et al., 2024; Levi, 2024; Schaeffer et al., 2025b; Huang et al., 2025b; Chen et al., 2024b; Du et al., 2025; Chen et al., 2025). These procedures are often paired with reasoning-oriented prompting and structured search that expand the candidate set before selection (Wei et al., 2022; Yao et al., 2023b). The work of Chen et al. (2024a) presented a theoretical model for majority voting in the premise of classification problems. More close to our work is the scaling law of Brown et al. (2024); Schaeffer et al. (2025b) for best-of- k strategy. For a given trained model, both these works explain some of the empirically observed patterns at inference. We study similar questions for the regression model and discuss trade-off between training and inference time compute taking into account the quality of the reward and the sampling process.

2 PROBLEM SETUP: BAYESIAN REGRESSION WITH REWARD-WEIGHTED SAMPLING

We start by introducing our solvable model.

2.1 TRAINING METHOD - PRIOR AND POSTERIOR DISTRIBUTION

We study a supervised regression setting with a linear teacher model that maps inputs to outputs and then adds observation noise. Throughout, let $\mathbf{x} \in \mathbb{R}^d$ denote an input vector drawn from a zero-mean Gaussian with covariance Σ , written $\mathbf{x} \sim \mathcal{N}(0, \Sigma)$. We assume $\text{Tr}(\Sigma) = \Theta_d(d)$ so that the total feature variance scales linearly with dimension; a canonical case is $\Sigma = \mathbf{I}$. The teacher parameter \mathbf{w}_T is taken to have norm $\|\mathbf{w}_T\|^2 = d$, and the output is given by:

$$y = \mathbf{w}_T \cdot \frac{\mathbf{x}}{\sqrt{d}} + \eta, \quad \eta \sim \mathcal{N}(0, \sigma^2). \quad (1)$$

Given a training set $\mathcal{D} = \{(\mathbf{x}^i, y^i)_{i=1}^n\}$ sampled i.i.d. from the teacher, we adopt a Bayesian linear regression perspective with an isotropic Gaussian prior on the weights, $\mathcal{N}(0, \gamma^2 \mathbf{I})$. Bayes' rule yields the posterior distribution over weights:

$$p(\mathbf{w}|\mathcal{D}) = \frac{p(\mathcal{D}|\mathbf{w})p(\mathbf{w})}{p(\mathcal{D})}. \quad (2)$$

Predictions for a new test input \mathbf{x} are obtained by marginalizing the likelihood under this posterior, producing the *posterior predictive* distribution:

$$p(y|\mathbf{x}, \mathcal{D}) = \int d\mathbf{w} p(\mathbf{w}|\mathcal{D})p(y|\mathbf{x}, \mathbf{w}). \quad (3)$$

Next we state the standard result that makes predictive distribution explicit.

Remark 1. *Analytical formula for the posterior predictive is given by*

$$p(y|\mathbf{x}, \mathcal{D}) = \mathcal{N}\left(\boldsymbol{\mu} \cdot \frac{\mathbf{x}}{\sqrt{d}}, \frac{\mathbf{x}^\top \boldsymbol{\Omega} \mathbf{x}}{\sqrt{d}} + \sigma^2\right) \quad (4)$$

$$\boldsymbol{\mu} = \frac{1}{\sigma^2} \boldsymbol{\Omega} \sum_{i=1}^n y^i \frac{\mathbf{x}^i}{\sqrt{d}}, \quad \boldsymbol{\Omega}^{-1} = \frac{1}{\sigma^2} \sum_{i=1}^n \frac{\mathbf{x}^i}{\sqrt{d}} \frac{\mathbf{x}^i}{\sqrt{d}}^\top + \frac{1}{\gamma^2} \mathbf{I} \quad (5)$$

Proof-sketch. This is a standard result Bishop (2013).

2.2 INFERENCE-TIME SAMPLING AND THE REWARD MODEL

Suppose that we have a reward model that evaluates our predictions, $r(y, \mathbf{x})$. We will use this to generate an output with the following procedure:

Reward-Weighted Sampling

Require: input \mathbf{x} , posterior predictive $p(y | \mathbf{x}, \mathcal{D})$, reward r , temperature T , number of samples k

- 1: **for** $i \leftarrow 1$ to k **do**
- 2: sample $y_i \sim p(y | \mathbf{x}, \mathcal{D})$
- 3: $l_i \leftarrow \exp(r(y_i, \mathbf{x})/T)$
- 4: $q_i \leftarrow l_i / \sum_{j=1}^k l_j \quad (i = 1, \dots, k)$
- 5: Draw $I \sim \text{Categorical}(q_1, \dots, q_k)$
- 6: **return** $y_{\text{out}} \leftarrow y_I$

For simplicity, we will assume a reward given by

$$r(y, \mathbf{x}) = - \left(y - \mathbf{w}_R \cdot \frac{\mathbf{x}}{\sqrt{d}} \right)^2. \quad (6)$$

Note that $\mathbf{w}_R \neq \mathbf{w}_T$ in general. In realistic settings, this models the fact that LLM-as-a-Judge is not a perfect verifier. Hence, this settings will allow us to study the effect of the quality of the Judge on generalization error.

In this paper, we are interested in computing the generalization error of this model defined by

$$\delta = \mathbb{E}_{\mathbf{x}}(\delta(\mathbf{x})), \quad (7)$$

$$\delta(\mathbf{x}) = \mathbb{E}_{y_1, \dots, y_k} \left[\frac{\sum_{i=1}^k (y_i - \mu_T(\mathbf{x}))^2 e^{-(y_i - \mu_R(\mathbf{x}))^2/T}}{\sum_{j=1}^k e^{-(y_j - \mu_R(\mathbf{x}))^2/T}} \right]. \quad (8)$$

Here we use the notation $\mu_T(\mathbf{x}) := \mathbf{w}_T \cdot \frac{\mathbf{x}}{\sqrt{d}}$, $\mu_R(\mathbf{x}) := \mathbf{w}_R \cdot \frac{\mathbf{x}}{\sqrt{d}}$.

3 ANALYSIS OF THE GENERALIZATION ERROR

In this section we analyze the high-dimensional behavior of the Bayesian regression model introduced above, with a particular focus on how inference-time sampling and the reward model shape the error.

3.1 ASYMPTOTIC BEHAVIOR OF THE GENERALIZATION ERROR VIA DETERMINISTIC EQUIVALENTS

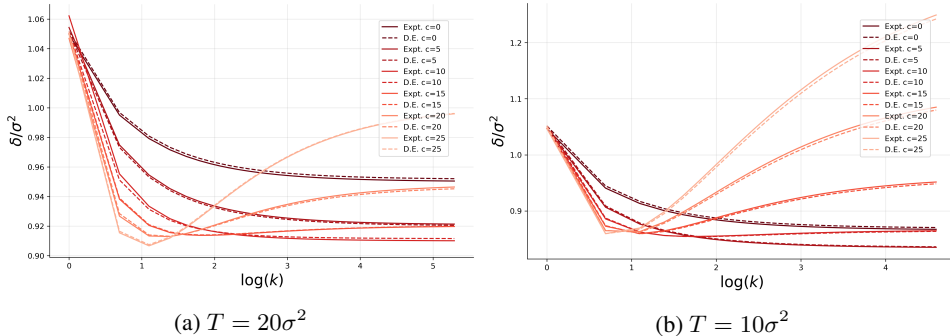


Figure 2: In the plot we have chosen $S = 1, \sigma = 10^{-4}, \gamma = 10^{-3}, n = 10^4, d = 10^1$ and sampled teacher weight $\mathbf{w}_T \sim \mathcal{N}(0, 2^2 \mathbf{I})$. We have parameterized the reward weight as follows: $\mathbf{w}_R = (1 + cR/(R + S^2))\mathbf{w}_T$. Solid and dashed lines correspond to the experimental results and the formula in Result 1 respectively. On y-axis we plot generalization error normalized by its natural scale set by the noise δ/σ^2 and in x-axis we plot the logarithm of the number of inference time samples $\log k$.

Before we get into the details of further theoretical analysis, we summarize the empirical findings in Figure 2 and compare with results of Result 1. When the reward is sufficiently accurate—formally, when $\|\mathbf{w}_R - \mathbf{w}_T\|/\|\mathbf{w}_T\|$ is small—the generalization error δ decreases *monotonically* with the number of inference-time samples k . We denote by \mathcal{R} (highlighted in red in Figure 1) the region of reward weights exhibiting this monotonic behavior. Notably, within \mathcal{R} the teacher reward is *not* optimal for fixed (k, T) ; i.e., $\mathbf{w}_R = \mathbf{w}_T$ does not minimize δ (see Figure 2a). Comparing figures 2a–2b, we note that the set \mathcal{R} shrinks as the temperature T decreases (see also Figure 1). Outside this set, in its complement \mathcal{R}^C (blue in Figure 1), Figure 2 shows that δ becomes *non-monotonic* in k , with a finite k beyond which increasing k worsens error. Consequently, for a fixed \mathbf{w}_R , lowering T can induce a transition from \mathcal{R} to \mathcal{R}^C ; equivalently, at fixed k there may exist an *optimal* temperature T that minimizes δ (confirmed in Figure 5). In the high dimensional setting, deterministic-equivalents simplify the predictive mean and variance by m and $\Sigma = s^2$ as follows:

Result 1. In the limit of $d, n \rightarrow \infty$, with $\alpha = d/n < 1$ fixed, for sufficiently small noise scale, i.e., there exists $\sigma_c(\alpha, R)$ such that for $\sigma \ll \sigma_c(\alpha, R)$, the generalization error is given by

$$\delta(\mathbf{x}) = \mathbb{E} \left[\frac{\sum_{i=1}^k (y_i - \mu_T(\mathbf{x}))^2 e^{-(y_i - \mu_R(\mathbf{x}))^2/T}}{\sum_{j=1}^k e^{-(y_j - \mu_R(\mathbf{x}))^2/T}} \right], \quad (9)$$

to the leading order in σ . Here the expectation is over $y_i \sim \mathcal{N}(m(\mathbf{x}), s(\mathbf{x})^2)$, $i = 1, 2, \dots, k$. The posterior predictive has a mean $m(\mathbf{x})$ and variance $\Sigma(\mathbf{x}) = s(\mathbf{x})^2$ as follows

$$m(\mathbf{x}) = \frac{\mathbf{x}}{\sqrt{d}}^\top \mathbf{A}_R \mathbf{w}_T, \quad s(\mathbf{x})^2 = \sigma^2 + \gamma^2 \frac{\mathbf{x}}{\sqrt{d}}^\top \mathbf{B}_R \frac{\mathbf{x}}{\sqrt{d}}. \quad (10)$$

The matrices $\mathbf{A}_R, \mathbf{B}_R$ are given by

$$\mathbf{A}_R := \Sigma(\Sigma + R\mathbf{I})^{-1}, \quad \mathbf{B}_R := R(\Sigma + R\mathbf{I})^{-1} = \mathbf{I} - \mathbf{A}_R. \quad (11)$$

and the renormalized ridge R is given by

$$\hat{R} = R \left(1 - \alpha m_\Sigma(R) \right) = \frac{\sigma^2}{\gamma^2} \alpha, \quad m_\Sigma(R) := \frac{1}{d} \text{Tr}[\Sigma(\Sigma + R\mathbf{I})^{-1}]. \quad (12)$$

Proof-sketch. See appendix B for more details.

In this paper we will focus on the simple setup where $\Sigma = S^2 \mathbf{I}$. In this case we can explicitly solve for the renormalized ridge as follows

$$R = \frac{1}{2} S^2 \left(\frac{d}{n} + \frac{\hat{R}}{S^2} - 1 + \left(\left(1 - \frac{d}{n} - \frac{\hat{R}}{S^2} \right)^2 + \frac{4\hat{R}}{S^2} \right)^{\frac{1}{2}} \right). \quad (13)$$

In addition in this case the matrices $\mathbf{A}_R, \mathbf{B}_R$ are proportional to identity matrix

$$\mathbf{A}_R := \frac{S^2}{R + S^2} \mathbf{I}, \quad \mathbf{B}_R := \frac{R}{R + S^2} \mathbf{I}. \quad (14)$$

These expressions are going to be useful in the later sections to have close form expression of generalization error δ in various parameter domains of interest.

3.2 HIGH- AND LOW-TEMPERATURE BEHAVIOR OF THE GENERALIZATION ERROR

We now provide a theoretical account of these phenomena. In this section, we present two results that will help us gain insight later into generalization error behavior. Specifically, we analyze δ in two complementary regimes of the reward temperature: (i) a high-temperature (weak-reward) expansion, where the selection reweighting is perturbative, and (ii) a low-temperature (“best-of- k ”) regime, where selection concentrates on high-reward samples and extreme-value effects dominate. The next two results formalize these regimes.

In the limit of an ample amount of data $d/n \rightarrow 0$ with a flat prior $\sigma/\gamma \rightarrow 0$, the temperature scale is controlled by $s^2 \approx \sigma^2$. In the high-temperature limit we present the following result.

Result 2 (High- T expansion). *For temperature much larger than the posterior predictive’s variance, i.e., $T \gg s(\mathbf{x})^2$ the expectation value of the error can be organized as a series as follows*

$$\begin{aligned} \delta(\mathbf{x}) &= \Delta_T(\mathbf{x})^2 + s^2(\mathbf{x}) \\ &+ \sum_{l=1}^3 (-1)^l \frac{C_l(\mathbf{x})}{t(\mathbf{x})^l} \prod_{i=1}^l \left(1 - \frac{i}{k} \right) + \mathcal{O}(t(\mathbf{x})^{-4}) \end{aligned} \quad (15)$$

Where we have defined $t(\mathbf{x}) = \frac{T}{2s(\mathbf{x})^2}$ and

$$\begin{aligned} C_l(\mathbf{x}) &= 2\Delta_T(\mathbf{x})\Delta_R(\mathbf{x}) + s^2(\mathbf{x}) + (l-1)\Delta_R(\mathbf{x})^2 \\ \Delta_T(\mathbf{x}) &:= m(\mathbf{x}) - \mu_T(\mathbf{x}), \quad \Delta_R(\mathbf{x}) := m(\mathbf{x}) - \mu_R(\mathbf{x}). \end{aligned} \quad (16)$$

All other quantities are as in Result 1.

Proof-sketch. Let z denote the partition function over k i.i.d. draws from $p(y|x, \mathcal{D})$ with quadratic reward; expand $\mathbb{E} \log z$ around $\mathbb{E} z$ via a controlled cumulant expansion for $t \gg 1$. The $1/t, 1/t^2$ and $1/t^3$ terms produce the $C_1(\mathbf{x}), C_2(\mathbf{x})$ and $C_3(\mathbf{x})$ structure; substituting the deterministic equivalents for m, Σ converts it to the form mentioned in the Result. See Appendix C for the details.

Now we turn to best-of- k setting, given by the $T \rightarrow 0$ limit, and present our theoretical finding below.

Result 3 (Low- T best-of- k sampling). *When we have access to the exact teacher weight $\mathbf{w}_R = \mathbf{w}_T = \mathbf{w}$, the leading order result for $T \rightarrow 0$ followed by $k \rightarrow \infty$ is given by*

$$\delta(\mathbf{x}) = \frac{\pi}{k^2} \left[s^2(\mathbf{x}) \exp\left(\frac{\Delta_T(\mathbf{x})^2}{s^2(\mathbf{x})}\right) \right] \quad (17)$$

All the quantities are as in Result 1 and Result 2.

Proof-sketch. At $T = 0$, the softmax reduces to a minimum of chi-squared random variables. This is governed by the Weibull distribution at large k according to extreme value theory. Finally, substituting the deterministic equivalents for m, Σ and evaluating the expectation value gives the generalization error mentioned in the Result. See Appendix 11 for details.

Note that the low-temperature scaling of δ with the number of inference time samples k is independent of the amount of the amount of training data. These theoretical results are compared with the experiment in Figure 6, Figure 7.

3.3 OPTIMAL REWARD MAY DIFFER FROM THE TEACHER

Naively, one might expect that the optimal reward, one that leads to the best generalization error, is given by the teacher itself. However, Figure 3 shows that this may not always be true. Here, we compare the generalization error achieved when the reward weight equals the teacher ($\mathbf{w}_R = \mathbf{w}_T$) versus when it differs, across different values of k and T . The plot reveals a consistent pattern: when \mathbf{w}_R is close to \mathbf{w}_T , the error is *lower* when the reward weight is *slightly shifted* away from the teacher. This additional shift required for the optimal reward grows systematically with the temperature scale T .

We can get insight into this behavior exploiting our Result 2. By setting the first derivative of $\delta(\mathbf{x})$, given in Result 2, with respect to \mathbf{w}_R to zero, we arrive at the following conclusion:

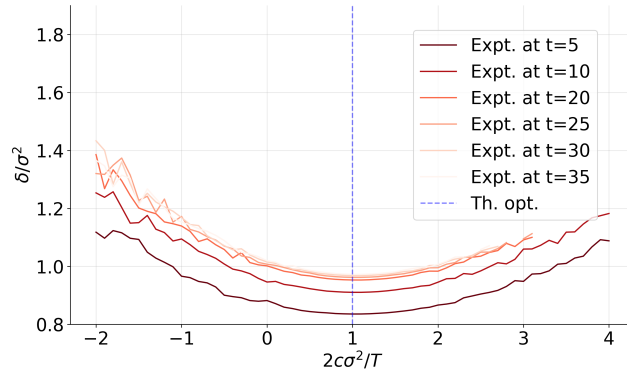


Figure 3: In the plot we have chosen $S = 1, \sigma = 10^{-4}, \gamma = 10^{-3}, n = 10^4, d = 10, k = 50$ and used the following parameterization $\mathbf{w}_R = (1 + cR/(R + S^2))\mathbf{w}_T$ and sampled $\mathbf{w}_T \sim \mathcal{N}(0, 2^2 \mathbf{I})$. This plot shows dependence of δ on c for various values of T at fixed k . We see that δ is minimized at $c \approx T/(2\sigma^2)$ as expected from Remark 2.

Remark 2. *There exists an optimal reward weight that differs from the teacher weight by the following formula*

$$\mathbf{w}_R(\mathbf{x}) = \mathbf{w}_T + \left(\frac{k}{k-2} t(\mathbf{x}) \right) \mathbf{B}_R \mathbf{w}_T \quad (18)$$

This formula provides a controlled approximation in the domain stated in Result 2 as long as

$$\frac{\|\mathbf{w}_R(\mathbf{x}) - \mathbf{w}_T\|}{\|\mathbf{w}_T\|} \ll 1. \quad (19)$$

The Remark also quantifies the empirically observed fact that as T increases, the optimal \mathbf{w}_R moves proportionally away from \mathbf{w}_T .

3.4 THERE EXISTS AN OPTIMAL NUMBER FOR INFERENCE-TIME SAMPLES

Figure 4 shows that when the reward weight \mathbf{w}_R is sufficiently misaligned from the teacher \mathbf{w}_T , the test error as a function of the number of inference samples k is *non-monotonic*: it first decreases (benefiting from a better draw among k candidates) and then *increases* beyond an optimal value of k . We can get some more insight into this behavior by the following Remark.

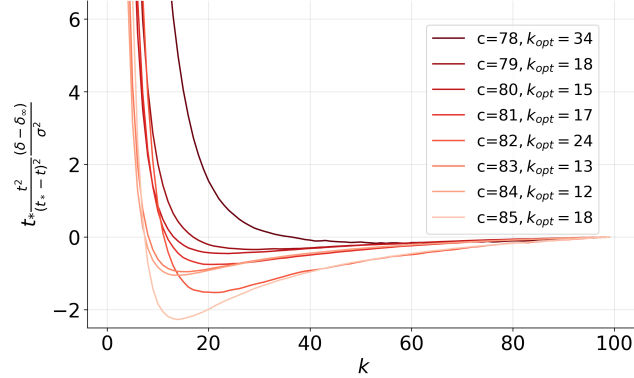


Figure 4: In the plot we have chosen $S = 1, \sigma = 10^{-4}, \gamma = 10^{-3}, n = 10^4, d = 10, T = 200\sigma^2$ and used the following parameterization $\mathbf{w}_R = (1 + cR/(R + S^2))\mathbf{w}_T$ and sampled $\mathbf{w}_T \sim \mathcal{N}(0, 2^2\mathbf{I})$. We plot the scaled value of $\delta - \delta_\infty, \delta_\infty \approx \delta_{k=100}$ as a function of k for various values of c . This shows existence of an optimal value of k - theoretical prediction for it is denoted as k_{opt} as given in Remark 3.

Remark 3. *There exists an optimal value of inference samples k , when Result 2 is valid and*

$$t < \frac{3C_2(\mathbf{x})}{C_1(\mathbf{x})} \equiv t_*, \quad C_1(\mathbf{x}) > 0, \quad C_2(\mathbf{x}) > 0 \quad (20)$$

In this case, as we increase k the error decreases until when we reach

$$k = \left\lceil \frac{4}{3} \frac{t_*}{t_* - t} \right\rceil \approx \frac{2t_*}{t_* - t} \quad (21)$$

and far beyond this, increase in k increases the error. For larger values of t , increase in k always decreases error.

Proof-sketch. This is obtained by setting the first derivative of $\delta(\mathbf{x})$, given in Result 2, with respect to k to zero.

Note that above Remark only applies when $t \gg 1$ and $t < 3C_2/C_1$. But when \mathbf{w}_R is sufficiently close to \mathbf{w}_T , $C_2/C_1 \sim 1$. When \mathbf{w}_R is sufficiently close to \mathbf{w}_T , increase in k decreases the error δ since in this case above Remark does not apply. Whereas when \mathbf{w}_R is sufficiently far from \mathbf{w}_T (C_2/C_1 becomes larger since Δ_R grows), above Remark shows existence of an optimal value for k .

3.5 THERE EXISTS AN OPTIMAL TEMPERATURE FOR REWARD SAMPLING

Figure 5 examines generalization δ error as a function of temperature T at fixed number of inference time samples k . Empirically, the generalization error exhibits a clear local minimum around a critical value of T , rather than decreasing or increasing monotonically. Interpreting this through the

high- T expansion, the minimum corresponds to a particular balance between the first- and second-order correction terms governed by C_1 and C_2 . Temperature T controls how sharply the selection favors high-reward samples among the k candidates. At very high temperatures, selection is nearly uniform and the benefits of the reward model are muted; at very low temperatures, selection becomes too aggressive and can over-amplify any mismatch between \mathbf{w}_R and \mathbf{w}_T , increasing error. The optimal temperature thus trades off these effects. It scales linearly with Σ and grows with misspecification via C_2/C_1 . The location of the optimal temperature for given k, \mathbf{w}_R is determined from the theoretical result below:

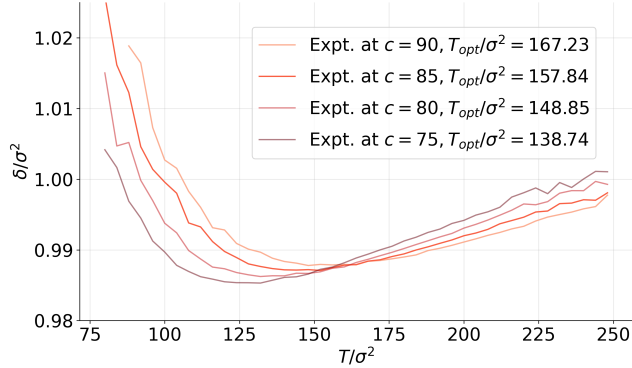


Figure 5: In the plot we have chosen $S = 1, \sigma = 10^{-4}, \gamma = 10^{-3}, n = 10^4, d = 10$ and used the following parameterization $\mathbf{w}_R = (1 + cR/(R + S^2))\mathbf{w}_T$ and sampled $\mathbf{w}_T \sim \mathcal{N}(0, 2^2\mathbf{I})$. This plot shows existence of an optimal value of temperature T at fixed $k = 50$. For the optimal value, we find reasonable agreement with the theoretical prediction in in Remark 4.

Remark 4. For a given number of inference-time samples $k > 2$, training dataset size n and reward weight \mathbf{w}_R , there exists an optimal temperature for the rewarding process

$$t(\mathbf{x}) = 2 \left(1 - \frac{2}{k}\right) \frac{C_2(\mathbf{x})}{C_1(\mathbf{x})}, \quad C_1(\mathbf{x}) > 0, \quad C_2(\mathbf{x}) > 0 \quad (22)$$

This formula is valid in the domain stated in Result 2.

Proof-sketch. This is obtained by setting the first derivative of $\delta(\mathbf{x})$, given in Result 2, with respect to t to zero.

3.6 TEACHER-REWarded BEST-OF- k SHOWS POWER-LAW DECAY

The low- T result in Result 3 shows an inverse-quadratic k^{-2} decay of the error when the reward matches the teacher ($\mathbf{w}_R = \mathbf{w}_T$). Here we sharpen that statement by identifying a concrete, practically relevant parameter domain in which the leading-order constant in front of k^{-2} can be written in closed form. Explicit formula clarifies how dimensionality, sample size, noise, and prior scale combine in the low-temperature limit.

Remark 5. As a refinement of Result 3, consider the parameter regime

$$\frac{\gamma^2}{d} \text{Tr}(\mathbf{B}_R \Sigma) \ll \sigma^2.$$

In the low-temperature limit $T \rightarrow 0$ followed by $k \rightarrow \infty$, the leading-order generalization error for $\mathbf{w}_R = \mathbf{w}_T = \mathbf{w}$ is given by

$$\delta = \frac{\pi\sigma^2}{k^2} \frac{1}{\sqrt{1 - \frac{2}{\sigma^2 d} \mathbf{u}^\top \Sigma \mathbf{u}}}, \quad \mathbf{u} := \mathbf{B}_R \mathbf{w}$$

Proof-sketch. In this domain the \mathbf{x} -dependence of $s^2(\mathbf{x})$ is small relative to σ^2 and this allows us to reliably set $s^2(\mathbf{x}) \approx \sigma^2$ in Result 3 to evaluate the expectation value.

In the flat prior limit, i.e., $\gamma^2 \gg \sigma^2$, this regime corresponds to ample amount of data per dimension, i.e., $n \gg d$. For the isotropic sample covariance $\Sigma = S^2\mathbf{I}$ that we are analyzing in this paper, we have $\mathbf{u} = \frac{R}{R+S^2}\mathbf{w}$. In the limit of flat prior with ample amount of data, this further simplifies to $\mathbf{u} \approx (1/S^2)(\sigma^2/\gamma^2)(d/n)\mathbf{w}$. The Remark above shows as task difficulty increases, i.e., σ gets larger keeping other parameters fixed, generalization error δ and even the scaled generalization error δ/σ^2 increases.

3.7 TRADE-OFF BETWEEN TRAINING AND INFERENCE-TIME COMPUTE

In practice we often face a budget allocation decision: should additional compute be spent on *training* (e.g., acquiring/processing more samples n) or on *inference-time* (e.g., drawing more candidates k and selecting via the reward)? When the reward is well aligned with the teacher and we operate in the low-temperature regime, best-of- k style selection can substantially reduce error with relatively modest inference cost. The question is how this compares with the addition of more data.

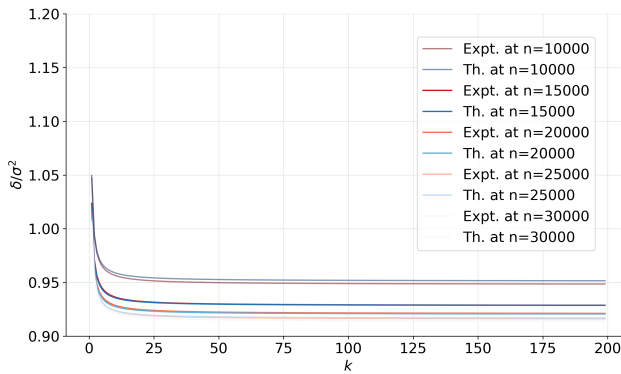


Figure 6: In the plot we have chosen $S = 1$, $\sigma = 10^{-4}$, $\gamma = 10^{-3}$, $d = 10$. We plot the theoretical (given in Result 2) and experimental value of δ and find good agreement for $\mathbf{w}_R = \mathbf{w}_T \sim \mathcal{N}(0, 2^2\mathbf{I})$. We see that in this domain scaling n higher is more useful compared to scaling k .

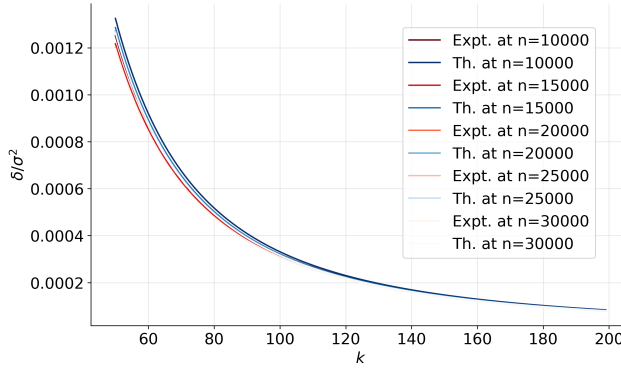


Figure 7: In the plot we have chosen $S = 1$, $\sigma = 10^{-4}$, $\gamma = 10^{-3}$, $d = 10$. We plot the theoretical (given in Result 3) and experimental value of δ at $T = 0$ and find good agreement for $\mathbf{w}_R = \mathbf{w}_T \sim \mathcal{N}(0, 2^2\mathbf{I})$. We see that in this domain scaling n higher is less useful compared to scaling k .

Remark 6. *Given access to exact teacher weight, it is beneficial to scale inference-time compute over adding more training samples in the following regime: consider $T \rightarrow 0$ followed by $k \rightarrow \infty$ with*

$$\frac{\gamma^2}{d} \text{Tr}(\mathbf{B}_R \Sigma) \ll \sigma^2, \quad R \ll \sigma^2 \quad (23)$$

That is within this domain,

$$\frac{\partial \log \delta}{\partial \log k} = -2, \quad \frac{\partial \log \delta}{\partial \log n} = -\frac{\alpha \partial_\alpha (\mathbf{u}^\top \Sigma \mathbf{u})}{\sigma^2 d - 2\mathbf{u}^\top \Sigma \mathbf{u}} \quad (24)$$

and hence

$$\left| \frac{\partial \log \delta}{\partial \log k} \right| \gg \left| \frac{\partial \log \delta}{\partial \log n} \right| \quad (25)$$

Proof-sketch. See Appendix E for details.

In the flat prior, i.e., $\gamma^2 \gg \sigma^2$, ample data limit, i.e., $n \gg d$, the second condition in the Remark quantifies prior quality - roughly speaking it dictates that when the prior γ is broad enough, inference time compute is beneficial over training time compute. For the isotropic sample covariance $\Sigma = S^2 \mathbf{I}$, putting back explicit formula for $\mathbf{u} \approx R/S^2 \mathbf{w} \approx (1/S^2)(\sigma^2/\gamma^2)(d/n)\mathbf{w}$ shows that

$$\frac{\partial \log \delta}{\partial \log n} = -2 \frac{\frac{\mathbf{w} \cdot \mathbf{w}}{d} \frac{1}{S^2} \frac{d^2 \sigma^2}{n^2 \gamma^4}}{1 - 2 \frac{\mathbf{w} \cdot \mathbf{w}}{d} \frac{1}{S^2} \frac{d^2 \sigma^2}{n^2 \gamma^4}} \quad (26)$$

In this case, under an even weaker condition $R^2 < \sigma^2$ already we see that scaling inference time is beneficial over scaling training compute. If σ increases keeping other parameters held fixed, the magnitude of the derivative of $\log \delta$ w.r.t. $\log n$ increases. Hence as the task becomes more difficult the advantage of inference time scaling degrades. The same statement holds true if γ decreases while other parameters are held fixed.

We empirically validate these results on advantages of inference-time scaling over training compute in Figure 7. It is clear from Figure 7 that fractional increase in k decreases generalization error δ more compared to the same fractional increase in n within the domain of parameters considered in the plot. However, inference-time scaling is not always advantageous over increasing training compute - we explain this in Figure 6. We conclude that when we have access to a good quality reward model and the task is easy enough, the addition of inference time compute is beneficial over additional training compute.

4 QUALITATIVE AGREEMENT WITH LARGE LANGUAGE MODEL REASONING

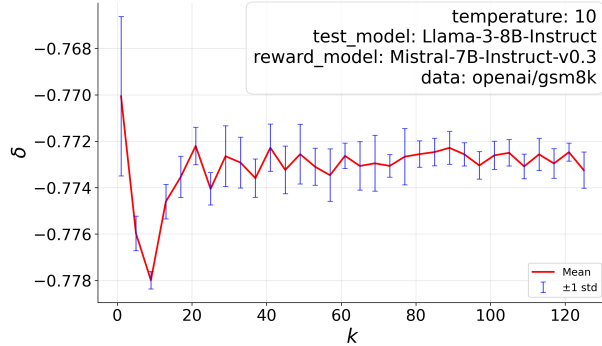


Figure 8: In the plot we have generated inference time samples from Llama-3-8B-Instruct. For each question and response pair we used Mistral-7B-Instruct-v0.3 (with simple/weak prompt). For generalization error we used the definition in equation 27. The variance in the graph is due to non-zero temperature of generation in Llama-3-8B-Instruct. Plot shows existence of an optimal value of k .

In this section, we discuss implications of our theoretical results for inference time scaling of large language models such as Llama-3-8B-Instruct, DeepSeek-R1-Distill-Qwen-1.5B on openai/gsm8k validation dataset (prompt included 8 chain of thought demonstrations). As the Judge model we used Mistral-7B-Instruct-v0.3 or Qwen2.5-Math-PRM-7B. For the details of experimental design see Appendix G.2.

In the linear model we have observed that the when the reward is not close to the teacher model there exists an optimal value of inference time samples. This fact has been observed in large language models in (Snell et al., 2025; Chen et al., 2024a). Figure 8 shows that there is a global minima in

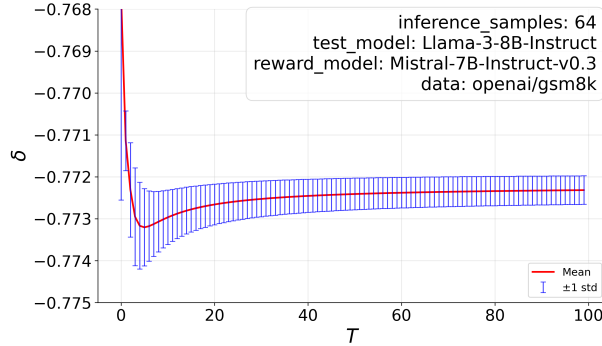


Figure 9: We use the same setup as in Figure. 8. Plot shows existence of an optimal value of T .

generalization error as a function of the inference time samples at fixed temperature, qualitatively validating our theoretical observation.

Our second observation is that there exists an optimal temperature for reward sampling. To the best of our knowledge this is a new observation and in this section we present experiments supporting it. For a given question \mathbf{x} we generate k responses $y_i, i = 1, 2, \dots, k$ from the large language model under study and use a judge language model to assign a reward $r(y_i, \mathbf{x})$ to i th response. The generalization error is defined by

$$\delta = -\mathbb{E}_{\mathbf{x}} \sum_{i=1}^k \frac{e^{\frac{r(y_i, \mathbf{x})}{T}}}{\sum_{j=1}^k e^{\frac{r(y_j, \mathbf{x})}{T}}} v(y_i, \mathbf{x}) \quad (27)$$

Here $v(y_i, \mathbf{x}) \in \{0, 1\}$ is 1 when the response is correct and 0 otherwise. When $T = 0$ this reduces to the best of k rewarding process. In Figure 9 we present experimental results confirming that there exists an optimal value of T .

In Figure 10 and Figure 11 we study the change of optimal values of k, T when the judge is changed from a weaker one to a stronger one by keeping the judge-LLM the same, but using a detailed prompt. During our study of the toy model, from Figure 4 we see that for a range of c , optimal value of k remained almost fixed. However, as the reward model became stronger, i.e., c is decreased, Figure 5 showed that optimal T also decreased. We see similar qualitative behavior from Figure 10 and 11 respectively.

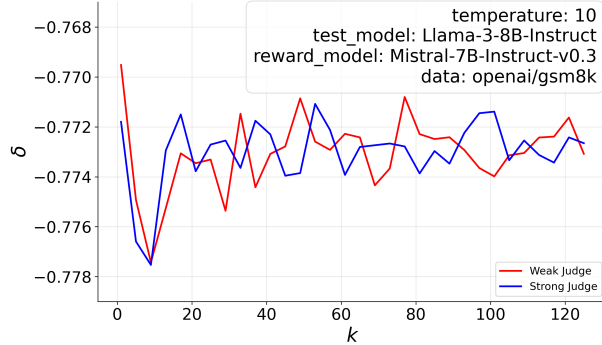


Figure 10: We use the same setup as in Figure. 8 with two different prompts for the reward model - a simple/weak prompt and a detailed/strong prompt (see Appendix G.2 for the details of the prompt). We call these weak and strong judge respectively. Plot shows behavior of the optimal value of k respectively under the change of judge. In the plot we have used a single generation from the Llama-3-8B-Instruct and kept the judge deterministic.

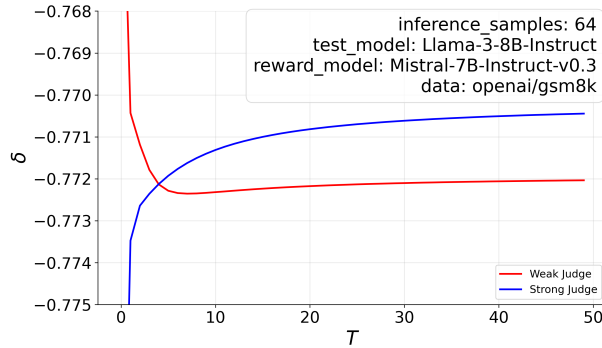


Figure 11: We use the same setup as in Figure 8 with two different prompts for the reward model as in Figure 10. Plot shows behavior of the optimal value of T under the change of judge.

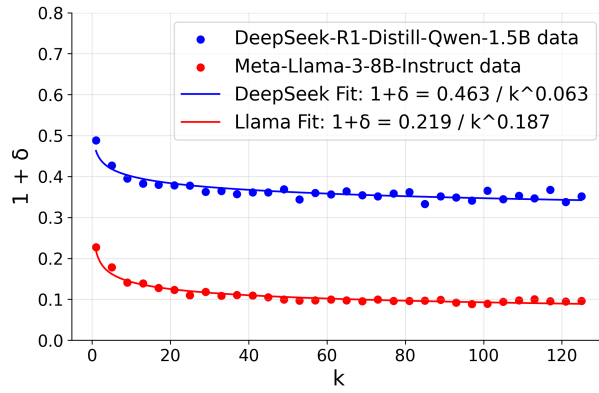


Figure 12: In this plot we plot the error $1+\delta$ of various base models vs k at fixed reward temperature $T = 0$ for nearly ideal reward model Qwen2.5-Math-PRM-7B. It is clear from the plot that the curves are well fitted by an effective scaling law similar to the result in Remark 5 except that the exponent of k is different.

In Figure 12 we use Qwen2.5-Math-PRM-7B as the reward model. This verifies each step of the reasoning and corresponds to nearly ideal reward. The plot shows that for best-of- k method the error decreases as a power law in inference time samples (almost monotonically). Similar result is established theoretically in Remark 5. Note that the judge in our case takes into account the reasoning process, not just final result of being correct or wrong and our metric is much different compared to pass@ k used in Brown et al. (2024); Schaeffer et al. (2025a).

5 CONCLUSION

We introduce a simple, solvable model to study how inference-time scaling works, where multiple candidate answers are generated and chosen using a reward-based selection process. Our analysis shows that when the reward model is well aligned with the task, increasing the number of inference time samples reliably improves generalization, but when it is misaligned, there is an optimal finite number of samples and an optimal temperature for selection. In the best-of- k setting with an ideal reward model, we identify a power law of generalization error and demonstrate when extra inference-time compute is more valuable than additional training. Finally, our experiments with modern language models on a math problem benchmark validate theoretical results.

In the linear setting, we show that the reward model that optimizes performance need not coincide with the teacher model. Leveraging properties of the trained predictor, we derive the optimal reward

model. By analogy, in large language models one can employ an auxiliary classifier that learns the model’s systematic weaknesses and selects which queries should be scored by the reward model; such classifier-guided reward shaping can further improve performance. A comprehensive study of these directions is left to future work.

We have also discussed trade-off between training and inference time scaling, analyzing it carefully in large language models is an important open question.

ACKNOWLEDGMENTS

I.H. is supported by DARPA grant AIQ-HR00112520041. C.P. is supported by an NSF CAREER Award (IIS-2239780), DARPA grants DIAL-FP-038 and AIQ-HR00112520041, the Simons Collaboration on the Physics of Learning and Neural Computation, and the William F. Milton Fund from Harvard University. I.H. and C.P. thank the Stanford Institute for Human-Centered Artificial Intelligence and the Kavli Institute for Theoretical Physics for its hospitality during the completion of this work. This work has been made possible in part by a gift from the Chan Zuckerberg Initiative Foundation to establish the Kempner Institute for the Study of Natural and Artificial Intelligence.

REFERENCES

Joel Hestness, Sharan Narang, Newsha Ardalani, Gregory Diamos, Heewoo Jun, Hassan Kianinejad, Md. Mostafa Ali Patwary, Yang Yang, and Yanqi Zhou. Deep learning scaling is predictable, empirically, 2017. URL <https://arxiv.org/abs/1712.00409>.

Jared Kaplan, Sam McCandlish, Tom Henighan, Tom B. Brown, Benjamin Chess, Rewon Child, Scott Gray, Alec Radford, Jeffrey Wu, and Dario Amodei. Scaling laws for neural language models, 2020. URL <https://arxiv.org/abs/2001.08361>.

Jordan Hoffmann, Sebastian Borgeaud, Arthur Mensch, Elena Buchatskaya, Trevor Cai, Eliza Rutherford, Diego de Las Casas, Lisa Anne Hendricks, Johannes Welbl, Aidan Clark, Tom Henigan, Eric Noland, Katie Millican, George van den Driessche, Bogdan Damoc, Aurelia Guy, Simon Osindero, Karen Simonyan, Erich Elsen, Jack W. Rae, Oriol Vinyals, and Laurent Sifre. Training compute-optimal large language models, 2022. URL <https://arxiv.org/abs/2203.15556>.

Xuezhi Wang, Jason Wei, Dale Schuurmans, Quoc V Le, Ed H. Chi, Sharan Narang, Aakanksha Chowdhery, and Denny Zhou. Self-consistency improves chain of thought reasoning in language models. In *The Eleventh International Conference on Learning Representations*, 2023.

Lianmin Zheng, Wei-Lin Chiang, Ying Sheng, Siyuan Zhuang, Zhanghao Wu, Yonghao Zhuang, Zi Lin, Zhuohan Li, Dacheng Li, Eric Xing, et al. Judging llm-as-a-judge with mt-bench and chatbot arena. *Advances in neural information processing systems*, 36:46595–46623, 2023.

Lunjun Zhang, Arian Hosseini, Hritik Bansal, Mehran Kazemi, Aviral Kumar, and Rishabh Agarwal. Generative verifiers: Reward modeling as next-token prediction. *arXiv preprint arXiv:2408.15240*, 2024.

Yangzhen Wu, Zhiqing Sun, Shanda Li, Sean Welleck, and Yiming Yang. Inference scaling laws: An empirical analysis of compute-optimal inference for problem-solving with language models. *arXiv preprint arXiv:2408.00724*, 2024.

Charlie Victor Snell, Jaehoon Lee, Kelvin Xu, and Aviral Kumar. Scaling LLM test-time compute optimally can be more effective than scaling parameters for reasoning. In *The Thirteenth International Conference on Learning Representations*, 2025.

Bradley Brown, Jordan Juravsky, Ryan Ehrlich, Ronald Clark, Quoc V. Le, Christopher Ré, and Azalia Mirhoseini. Large language monkeys: Scaling inference compute with repeated sampling. *arXiv preprint*, 2024.

Rylan Schaeffer, Joshua Kazdan, John Hughes, Jordan Juravsky, Sara Price, Aengus Lynch, Erik Jones, Robert Kirk, Azalia Mirhoseini, and Sanmi Koyejo. How do large language monkeys get their power (laws)?, 2025a. URL <https://arxiv.org/abs/2502.17578>.

Lingjiao Chen, Jared Quincy Davis, Boris Hanin, Peter Bailis, Ion Stoica, Matei Zaharia, and James Zou. Are more LLM calls all you need? towards the scaling properties of compound AI systems. In *The Thirty-eighth Annual Conference on Neural Information Processing Systems*, 2024a. URL <https://openreview.net/forum?id=m5106RRLgx>.

Audrey Huang, Adam Block, Qinghua Liu, Nan Jiang, Akshay Krishnamurthy, and Dylan J Foster. Is best-of-n the best of them? coverage, scaling, and optimality in inference-time alignment. *arXiv preprint arXiv:2503.21878*, 2025a.

William Saunders, Catherine Yeh, Jeff Wu, Steven Bills, Long Ouyang, Jonathan Ward, and Jan Leike. Self-critiquing models for assisting human evaluators. *arXiv preprint arXiv:2206.05802*, 2022.

Yixuan Weng, Minjun Zhu, Fei Xia, Bin Li, Shizhu He, Shengping Liu, Bin Sun, Kang Liu, and Jun Zhao. Large language models are better reasoners with self-verification. In *Findings of the Association for Computational Linguistics: EMNLP 2023*, pages 2550–2575, 2023.

Gonçalo Faria and Noah A Smith. Sample, don’t search: Rethinking test-time alignment for language models. *arXiv preprint arXiv:2504.03790*, 2025.

Weihua Du, Yiming Yang, and Sean Welleck. Optimizing temperature for language models with multi-sample inference. *arXiv preprint arXiv:2502.05234*, 2025.

Anders Krogh and John A Hertz. Generalization in a linear perceptron in the presence of noise. *Journal of Physics A: Mathematical and General*, 25(5):1135, 1992.

Lee H. Dicker. Ridge regression and asymptotic minimax estimation over spheres of growing dimension. *Bernoulli*, 22(1):1 – 37, 2016. doi: 10.3150/14-BEJ609. URL <https://doi.org/10.3150/14-BEJ609>.

Edgar Dobriban and Stefan Wager. High-dimensional asymptotics of prediction: Ridge regression and classification. *The Annals of Statistics*, 46(1):247 – 279, 2018. doi: 10.1214/17-AOS1549. URL <https://doi.org/10.1214/17-AOS1549>.

Preetum Nakkiran. More data can hurt for linear regression: Sample-wise double descent. *arXiv preprint arXiv:1912.07242*, 2019.

Madhu S Advani, Andrew M Saxe, and Haim Sompolinsky. High-dimensional dynamics of generalization error in neural networks. *Neural Networks*, 132:428–446, 2020.

Trevor Hastie, Andrea Montanari, Saharon Rosset, and Ryan J Tibshirani. Surprises in high-dimensional ridgeless least squares interpolation. *The Annals of Statistics*, 50(2):949–986, 2022.

Peter Sollich. Learning curves for Gaussian processes. *Advances in neural information processing systems*, 11, 1998.

Peter Sollich and Anason Halees. Learning curves for Gaussian process regression: Approximations and bounds. *Neural computation*, 14(6):1393–1428, 2002.

Blake Bordelon, Abdulkadir Canatar, and Cengiz Pehlevan. Spectrum dependent learning curves in kernel regression and wide neural networks. In *Proceedings of the 37th International Conference on Machine Learning*, volume 119 of *Proceedings of Machine Learning Research*, pages 1024–1034. PMLR, 2020. URL <https://proceedings.mlr.press/v119/bordelon20a.html>.

Abdulkadir Canatar, Blake Bordelon, and Cengiz Pehlevan. Spectral bias and task-model alignment explain generalization in kernel regression and infinitely wide neural networks. *Nature communications*, 12(1):2914, 2021.

Stefano Spigler, Mario Geiger, and Matthieu Wyart. Asymptotic learning curves of kernel methods: empirical data v.s. teacher-student paradigm. *Journal of Statistical Mechanics: Theory and Experiment*, (12):124001, 2020. doi: 10.1088/1742-5468/abc61d. URL <https://arxiv.org/abs/1905.10843>.

James B Simon, Madeline Dickens, Dhruva Karkada, and Michael Deweese. The eigenlearning framework: A conservation law perspective on kernel ridge regression and wide neural networks. *Transactions on Machine Learning Research*, 2023.

Bruno Loureiro, Cedric Gerbelot, Hugo Cui, Sebastian Goldt, Florent Krzakala, Marc Mezard, and Lenka Zdeborová. Learning curves of generic features maps for realistic datasets with a teacher-student model. *Advances in Neural Information Processing Systems*, 34:18137–18151, 2021.

Cosme Louart, Zhenyu Liao, and Romain Couillet. A random matrix approach to neural networks. *The Annals of Applied Probability*, 28(2):1190–1248, 2018.

Song Mei and Andrea Montanari. The generalization error of random features regression: Precise asymptotics and the double descent curve. *Communications on Pure and Applied Mathematics*, 75(4):667–766, 2022.

Ben Adlam and Jeffrey Pennington. The neural tangent kernel in high dimensions: Triple descent and a multi-scale theory of generalization. In *International Conference on Machine Learning*, pages 74–84. PMLR, 2020.

Stéphane d’Ascoli, Maria Refinetti, Giulio Biroli, and Florent Krzakala. Double trouble in double descent: Bias and variance (s) in the lazy regime. In *International Conference on Machine Learning*, pages 2280–2290. PMLR, 2020.

Stéphane d’Ascoli, Levent Sagun, and Giulio Biroli. Triple descent and the two kinds of overfitting: Where & why do they appear? *Advances in Neural Information Processing Systems*, 33:3058–3069, 2020.

Yasaman Bahri, Ethan Dyer, Jared Kaplan, Jaehoon Lee, and Utkarsh Sharma. Explaining neural scaling laws. In *International Conference on Learning Representations*, 2022. URL <https://openreview.net/forum?id=FvfV64rovny>. ICLR 2022.

Jacob A Zavatone-Veth and Cengiz Pehlevan. Learning curves for deep structured Gaussian feature models. In *Advances in Neural Information Processing Systems*, 2023a.

Oussama Dhiballah and Yue M Lu. A precise performance analysis of learning with random features. *arXiv preprint arXiv:2008.11904*, 2020.

Hong Hu and Yue M Lu. Universality laws for high-dimensional learning with random features. *IEEE Transactions on Information Theory*, 69(3):1932–1964, 2022.

Alexander Maloney, Daniel A. Roberts, and James Sully. A solvable model of neural scaling laws. 2022. doi: 10.48550/arXiv.2210.16859. URL <https://arxiv.org/abs/2210.16859>.

Francis Bach. High-dimensional analysis of double descent for linear regression with random projections. *SIAM Journal on Mathematics of Data Science*, 6(1):26–50, 2024.

Dan V Voiculescu, Ken J Dykema, and Alexandru Nica. *Free random variables*. American Mathematical Society, 1992.

A. Zee. Law of addition in random matrix theory. *Nuclear Physics B*, 474(3):726–744, 1996. ISSN 0550-3213. doi: [https://doi.org/10.1016/0550-3213\(96\)00276-3](https://doi.org/10.1016/0550-3213(96)00276-3). URL <https://www.sciencedirect.com/science/article/pii/0550321396002763>.

Theodor Misiakiewicz and Basil Saeed. A non-asymptotic theory of kernel ridge regression: deterministic equivalents, test error, and GCV estimator. *arXiv preprint arXiv:2403.08938*, 2024.

Alexander Atanasov, Jacob A. Zavatone-Veth, and Cengiz Pehlevan. Scaling and renormalization in high-dimensional regression, 2024. URL <https://arxiv.org/abs/2405.00592>.

James B. Simon, Blake Bordelon, Cengiz Pehlevan, and Michael R. DeWeese. The eigenlearning framework: A conservation law perspective on kernel regression and wide neural networks. 2021. URL <https://arxiv.org/abs/2110.03922>.

Blake Bordelon, Alexander Atanasov, and Cengiz Pehlevan. A dynamical model of neural scaling laws. In *Proceedings of the 41st International Conference on Machine Learning*, volume 235 of *Proceedings of Machine Learning Research*, pages 4345–4382. PMLR, 2024. URL <https://proceedings.mlr.press/v235/bordelon24a.html>.

Jacob A. Zavatone-Veth and Cengiz Pehlevan. Learning curves for deep structured gaussian feature models. In *Advances in Neural Information Processing Systems 36 (NeurIPS 2023)*, 2023b. URL https://proceedings.neurips.cc/paper_files/paper/2023/hash/85d456fd41f3eec83bd3b0c337037a0e-Abstract-Conference.html.

Elliot Paquette, Courtney Paquette, Lechao Xiao, and Jeffrey Pennington. 4+3 phases of compute-optimal neural scaling laws. In *Advances in Neural Information Processing Systems 37 (NeurIPS 2024)*, pages 16459–16537. Curran Associates, Inc., 2024. URL https://papers.neurips.cc/paper_files/paper/2024/hash/1dccfc3ee01871d05e33457c61037d59-Abstract-Conference.html.

Licong Lin, Jingfeng Wu, Sham M. Kakade, Peter L. Bartlett, and Jason D. Lee. Scaling laws in linear regression: Compute, parameters, and data. In *Advances in Neural Information Processing Systems 37 (NeurIPS 2024)*, 2024. URL https://proceedings.neurips.cc/paper_files/paper/2024/file/6fcblafcc1e9c2c82c82dddf03bcf0f6-Paper-Conference.pdf.

Blake Bordelon, Alexander Atanasov, and Cengiz Pehlevan. How feature learning can improve neural scaling laws. *Journal of Statistical Mechanics: Theory and Experiment*, 2025(8):084002, 2025.

Amrit Setlur, Nived Rajaraman, Sergey Levine, and Aviral Kumar. Scaling test-time compute without verification or rl is suboptimal. arXiv preprint, 2025.

Daman Arora and Andrea Zanette. Training language models to reason efficiently. *arXiv preprint arXiv:2502.04463*, 2025. URL <https://arxiv.org/abs/2502.04463>. v3, 19 May 2025.

Runze Liu, Junqi Gao, Jian Zhao, Kaiyan Zhang, Xiu Li, Binqing Qi, Wanli Ouyang, and Bowen Zhou. Can 1b llm surpass 405b llm? rethinking compute-optimal test-time scaling. arXiv preprint, 2025.

Shunyu Yao, Dian Yu, Jeffrey Zhao, Izhak Shafran, Tom Griffiths, Yuan Cao, and Karthik Narasimhan. Tree of thoughts: Deliberate problem solving with large language models. *Advances in neural information processing systems*, 36:11809–11822, 2023a.

Noam Levi. A simple model of inference scaling laws. *arXiv preprint arXiv:2410.16377*, 2024.

Rylan Schaeffer, Joshua Kazdan, John Hughes, Jordan Juravsky, Sara Price, Aengus Lynch, Erik Jones, Robert Kirk, Azalia Mirhoseini, and Sanmi Koyejo. How do large language monkeys get their power (laws)? *arXiv preprint arXiv:2502.17578*, 2025b.

Audrey Huang, Adam Block, Qinghua Liu, Nan Jiang, Akshay Krishnamurthy, and Dylan J. Foster. Is best-of-n the best of them? coverage, scaling, and optimality in inference-time alignment. arXiv preprint, 2025b.

Lingjiao Chen, Jared Quincy Davis, Boris Hanin, Peter Bailis, Ion Stoica, Matei Zaharia, and James Zou. Are more llm calls all you need? towards scaling laws of compound inference systems. arXiv preprint, 2024b.

Feng Chen, Allan Raventos, Nan Cheng, Surya Ganguli, and Shaul Druckmann. Rethinking fine-tuning when scaling test-time compute: Limiting confidence improves mathematical reasoning, 2025. URL <https://arxiv.org/abs/2502.07154>.

Jason Wei, Xuezhi Wang, Dale Schuurmans, and et al. Chain-of-thought prompting elicits reasoning in large language models. *arXiv preprint arXiv:2201.11903*, 2022.

Shunyu Yao, Dian Zhao, Nan Du Yu, Karthik Narasimhan Park, and Yuan Cao. Tree of thoughts: Deliberate problem solving with large language models. *arXiv preprint arXiv:2305.10601*, 2023b.

C.M. Bishop. *Pattern Recognition and Machine Learning*. Information science and statistics. Springer (India) Private Limited, 2013. ISBN 9788132209065. URL <https://books.google.com/books?id=HL4HrgEACAAJ>.

L. de Haan and A. Ferreira. *Extreme Value Theory: An Introduction*. Springer Series in Operations Research and Financial Engineering. Springer New York, 2007. ISBN 9780387344713. URL <https://books.google.com/books?id=t6tfXnykazEC>.

A REVIEW OF EXTREME VALUE STATISTICS

A.1 LIMIT LAWS FOR MAXIMA

Here we note some of the useful results in extreme value theory from de Haan and Ferreira (2007).

Result 4 (Fisher–Tippett–Gnedenko). *Let X_1, X_2, \dots be i.i.d. non-degenerate random variables with distribution function F , i.e., $F(x) = \mathbb{P}(X \leq x)$, and let $M_n = \max\{X_1, \dots, X_n\}$. If there exist normalising constants $a_n > 0$ and $b_n \in \mathbb{R}$ and a non-degenerate distribution function H such that*

$$\mathbb{P}\left(\frac{M_n - b_n}{a_n} \leq x\right) \xrightarrow{n \rightarrow \infty} H(x)$$

then H must be (up to affine change of variable) one of the three extreme value distributions:

$$\begin{aligned} \text{Fr\'echet } (\alpha > 0) : \quad \Phi_\alpha(x) &= \begin{cases} 0, & x \leq 0, \\ \exp\{-x^{-\alpha}\}, & x > 0, \end{cases} \\ \text{Weibull } (\alpha > 0) : \quad \Psi_\alpha(x) &= \begin{cases} \exp\{-(x)^{\alpha}\}, & x \leq 0, \\ 1, & x > 0, \end{cases} \\ \text{Gumbel} : \quad \Lambda(x) &= \exp\{-e^{-x}\}, \quad x \in \mathbb{R}. \end{aligned}$$

A.2 MAXIMUM DOMAINS OF ATTRACTION AND NORMING CONSTANTS

Definition 5 (Maximum domain of attraction). *We say F belongs to the maximum domain of attraction of H (write $F \in \text{MDA}(H)$) if there exist constants $a_n > 0, b_n \in \mathbb{R}$ such that*

$$\lim_{n \rightarrow \infty} F^n(a_n x + b_n) = H(x)$$

Remark 7 (Characterisation via exceedance rates). *Let H be a (standard) extreme value distribution. Then $F \in \text{MDA}(H)$ with norming constants $a_n > 0, b_n \in \mathbb{R}$ if and only if*

$$\lim_{n \rightarrow \infty} n(1 - F(a_n x + b_n)) = -\ln H(x)$$

For later convenience we define right endpoint $x_F := \sup\{x : F(x) < 1\}$, complementary distribution function $\bar{F}(x) := 1 - F(x)$ and quantile function $F^\leftarrow(t) = \inf\{x \in \mathbb{R} : F(x) \geq t\}$.

A.2.1 THE MAXIMUM DOMAIN OF ATTRACTION OF THE FR\'ECHET DISTRIBUTION

Result 6 (MDA of Fr\'echet). *Let F have a finite right endpoint $x_F = \infty$ and assume there exists $z < x_F$ such that F is differentiable in (z, x_F) . The following statements are equivalent:*

(i) F satisfies von Mises condition, i.e.,

$$\lim_{x \rightarrow x_F^-} \frac{x F'(x)}{1 - F(x)} = \alpha > 0 \tag{28}$$

(ii) $F \in \text{MDA}(\Phi_\alpha)$ with a possible choice of norming constants

$$b_n = 0, \quad a_n = F^\leftarrow\left(1 - \frac{1}{n}\right),$$

A.2.2 THE MAXIMUM DOMAIN OF ATTRACTION OF THE WEIBULL DISTRIBUTION

Result 7 (MDA of Weibull). *Let F have a finite right endpoint $x_F < \infty$ and assume there exists $z < x_F$ such that F is differentiable in (z, x_F) . The following statements are equivalent:*

(i) F satisfies von Mises condition, i.e.,

$$\lim_{x \rightarrow x_F^-} \frac{(x_F - x) F'(x)}{1 - F(x)} = \alpha > 0 \quad (29)$$

(ii) $F \in \text{MDA}(\Psi_\alpha)$ with a possible choice of norming constants

$$b_n = x_F, \quad a_n = x_F - F^\leftarrow\left(1 - \frac{1}{n}\right),$$

A.2.3 THE MAXIMUM DOMAIN OF ATTRACTION OF THE GUMBEL DISTRIBUTION

Result 8 (MDA of Gumbel). *Let F be a distribution with right endpoint $x_F \leq \infty$, and assume there exists $z < x_F$ such that F is at least twice differentiable in (z, x_F) . Define auxiliary function $a(x) = \bar{F}(x)/F'(x)$. The following statements are equivalent:*

(i) F is a von Mises function, i.e.,

$$\lim_{x \rightarrow x_F^-} a'(x) = 0$$

(ii) $F \in \text{MDA}(\Lambda)$ with a possible choice of norming constants

$$b_n = F^\leftarrow(1 - 1/n), \quad a_n = a(b_n)$$

B PROOF OF RESULT 1

Result 9. *In the limit of $d, n \rightarrow \infty$, with $\alpha = d/n < 1$ fixed, for sufficiently small noise scale, i.e., there exists $\sigma_c(\alpha, R)$ such that for $\sigma \ll \sigma_c(\alpha, R)$, the generalization error is given by*

$$\delta = \mathbb{E}_{\mathbf{x}} \mathbb{E}_{y_1, y_2, \dots} \left[\frac{\sum_{i=1}^k (y_i - \mu_T(\mathbf{x}))^2 e^{-(y_i - \mu_R(\mathbf{x}))^2/T}}{\sum_{j=1}^k e^{-(y_j - \mu_R(\mathbf{x}))^2/T}} \right], \quad (30)$$

to the leading order in σ . Here the expectation is over $\mathbf{x} \sim \mathcal{N}(0, \Sigma)$, $y_i \sim \mathcal{N}(m(\mathbf{x}), s(\mathbf{x})^2)$, $i = 1, 2, \dots, k$. The posterior predictive has mean $m(\mathbf{x})$ and variance $\Sigma(\mathbf{x}) = s(\mathbf{x})^2$ as follows

$$m(\mathbf{x}) = \frac{\mathbf{x}^\top}{\sqrt{d}} \mathbf{A}_R \mathbf{w}_T, \quad s(\mathbf{x})^2 = \sigma^2 + \gamma^2 \frac{\mathbf{x}^\top}{\sqrt{d}} \mathbf{B}_R \frac{\mathbf{x}}{\sqrt{d}}. \quad (31)$$

The matrices $\mathbf{A}_R, \mathbf{B}_R$ are given by

$$\mathbf{A}_R := \Sigma(\Sigma + R\mathbf{I})^{-1}, \quad \mathbf{B}_R := R(\Sigma + R\mathbf{I})^{-1} = \mathbf{I} - \mathbf{A}_R. \quad (32)$$

and the renormalized ridge R is given by

$$\begin{aligned} \hat{R} &= R \left(1 - \alpha m_\Sigma(R)\right) = \frac{\sigma^2}{\gamma^2} \alpha, \\ m_\Sigma(R) &:= \frac{1}{d} \text{Tr}[\Sigma(\Sigma + R\mathbf{I})^{-1}]. \end{aligned} \quad (33)$$

Proof-sketch. Let the empirical covariance be $\hat{\Sigma} := \frac{1}{n} \sum_{i=1}^n \mathbf{x}^i \mathbf{x}^{i\top}$, then

$$\Omega = \sigma^2 \alpha \left(\hat{\Sigma} + \hat{R} \mathbf{I} \right)^{-1}, \quad \hat{R} := \frac{\sigma^2}{\gamma^2} \alpha. \quad (34)$$

The mean of the predictive is given by

$$m(\mathbf{x}) = \boldsymbol{\mu}^\top \frac{\mathbf{x}}{\sqrt{d}} = \frac{1}{\sigma^2} \frac{\mathbf{x}^\top}{\sqrt{d}} \boldsymbol{\Omega} \sum_{i=1}^n y^i \frac{\mathbf{x}^i}{\sqrt{d}} \quad (35)$$

$$= \frac{\mathbf{x}^\top}{\sqrt{d}} \left(\mathbf{I} - \frac{1}{\gamma^2} \boldsymbol{\Omega} \right) \mathbf{w}_T + \frac{1}{\sigma^2} \frac{\mathbf{x}^\top}{\sqrt{d}} \boldsymbol{\Omega} \sum_{i=1}^n \eta^i \frac{\mathbf{x}^i}{\sqrt{d}}, \quad (36)$$

Now we use $\mathbf{I} - (1/\gamma^2)\Omega = \mathbf{I} - \hat{R}(\hat{\Sigma} + \hat{R}\mathbf{I})^{-1} = \hat{\Sigma}(\hat{\Sigma} + \hat{R}\mathbf{I})^{-1}$ to get

$$m(\mathbf{x}) = \langle \hat{\Sigma}(\hat{\Sigma} + \hat{R}\mathbf{I})^{-1}\mathbf{w}_T, \frac{\mathbf{x}}{\sqrt{d}} \rangle + \frac{1}{\sigma^2} \frac{\mathbf{x}^\top}{\sqrt{d}} \Omega \sum_{i=1}^n \eta^i \frac{\mathbf{x}^i}{\sqrt{d}}, \quad (37)$$

Conditioned test data $[\mathbf{x}^1, \dots, \mathbf{x}^n]$ and the test \mathbf{x} , the vector $\sum_{i=1}^n \eta^i \frac{\mathbf{x}^i}{\sqrt{d}}$ has zero mean with conditional covariance $\sigma^2 \sum_{i=1}^n \frac{\mathbf{x}^i}{\sqrt{d}} \frac{\mathbf{x}^i}{\sqrt{d}}^\top$. When σ is sufficiently small we can ignore this contribution. We will present a detailed justification of this fact below.

The variance of the predictive can be simplified to

$$\begin{aligned} s^2(\mathbf{x}) &= \frac{\mathbf{x}^\top}{\sqrt{d}} \Omega \frac{\mathbf{x}}{\sqrt{d}} + \sigma^2 = \frac{\mathbf{x}^\top}{\sqrt{d}} [\sigma^2 \alpha(\hat{\Sigma} + \hat{R}\mathbf{I})^{-1}] \frac{\mathbf{x}}{\sqrt{d}} + \sigma^2 \\ &= \gamma^2 \frac{\mathbf{x}^\top}{\sqrt{d}} [\hat{R}(\hat{\Sigma} + \hat{R}\mathbf{I})^{-1}] \frac{\mathbf{x}}{\sqrt{d}} + \sigma^2, \end{aligned} \quad (38)$$

There exists a $R > 0$ as defined in the Result such that, for any vectors u, v with bounded norms,

$$u^\top [\hat{\Sigma}(\hat{\Sigma} + \hat{R}\mathbf{I})^{-1}] v \xrightarrow{p} u^\top [\Sigma(\Sigma + R\mathbf{I})^{-1}] v = u^\top \mathbf{A}_R v, \quad (39)$$

$$u^\top [\hat{R}(\hat{\Sigma} + \hat{R}\mathbf{I})^{-1}] v \xrightarrow{p} u^\top [R(\Sigma + R\mathbf{I})^{-1}] v = u^\top \mathbf{B}_R v. \quad (40)$$

Applying equation 39 to equation 37, yields

$$m(\mathbf{x}) \xrightarrow{p} \frac{\mathbf{x}^\top}{\sqrt{d}} \mathbf{A}_R \mathbf{w}_T$$

Applying equation 40 to equation 38 with $u = v = \frac{\mathbf{x}}{\sqrt{d}}$ yields

$$s^2(\mathbf{x}) \xrightarrow{p} \sigma^2 + \gamma^2 \frac{\mathbf{x}^\top}{\sqrt{d}} \mathbf{B}_R \frac{\mathbf{x}}{\sqrt{d}}.$$

Now we turn to give a precise condition for when it is suitable to drop the noise term. Define

$$Z(\mathbf{x}) := \frac{1}{\sigma^2} \frac{\mathbf{x}^\top}{\sqrt{d}} \Omega \sum_{i=1}^n \eta^i \frac{\mathbf{x}^i}{\sqrt{d}}. \quad (41)$$

Then, in the proportional limit $d, n \rightarrow \infty$ with α fixed, the variance of the label-noise term $Z(\mathbf{x})$ admits the deterministic equivalent

$$\begin{aligned} \text{Var}(Z(\mathbf{x})) &\xrightarrow[d, n \rightarrow \infty]{} \sigma^2 \frac{\alpha m_{\Sigma}^{(2)}(R)}{1 - \alpha m_{\Sigma}^{(2)}(R)}, \\ m_{\Sigma}^{(2)}(R) &:= \frac{1}{d} \text{Tr}[\Sigma^2(\Sigma + R\mathbf{I})^{-2}] \end{aligned} \quad (42)$$

Next we explain this. Conditioned on the training inputs $\{\mathbf{x}^i\}_{i=1}^n$ and the test point \mathbf{x} . Using equation 41 and the fact that $\boldsymbol{\eta} = (\eta^1, \dots, \eta^n)^\top \sim \mathcal{N}(0, \sigma^2 \mathbf{I}_n)$ is independent of \mathcal{D} and \mathbf{x} , we have

$$Z(\mathbf{x}) = \frac{1}{\sigma^2} \frac{\mathbf{x}^\top}{\sqrt{d}} \Omega \sum_{i=1}^n \eta^i \frac{\mathbf{x}^i}{\sqrt{d}} = \frac{1}{\sigma^2} \frac{\mathbf{x}^\top}{\sqrt{d}} \Omega \tilde{X}^\top \boldsymbol{\eta},$$

where $\tilde{X} \in \mathbb{R}^{n \times d}$ has rows $\frac{\mathbf{x}^i}{\sqrt{d}}^\top$. Hence

$$\mathbb{E}[Z(\mathbf{x}) \mid \mathcal{D}, \mathbf{x}] = 0,$$

and

$$\text{Cov}(\tilde{X}^\top \boldsymbol{\eta} \mid \mathcal{D}) = \mathbb{E}[\tilde{X}^\top \boldsymbol{\eta} \boldsymbol{\eta}^\top \tilde{X} \mid \mathcal{D}] = \sigma^2 \tilde{X}^\top \tilde{X} = \sigma^2 \sum_{i=1}^n \frac{\mathbf{x}^i}{\sqrt{d}} \frac{\mathbf{x}^i}{\sqrt{d}}^\top.$$

Therefore

$$\begin{aligned}
\text{Var}(Z(\mathbf{x}) \mid \mathcal{D}, \mathbf{x}) &= \frac{1}{\sigma^4} \frac{\mathbf{x}^\top}{\sqrt{d}} \boldsymbol{\Omega} \text{Cov}(\tilde{\mathbf{X}}^\top \boldsymbol{\eta} \mid \mathcal{D}) \boldsymbol{\Omega}^\top \frac{\mathbf{x}}{\sqrt{d}} \\
&= \frac{1}{\sigma^4} \frac{\mathbf{x}^\top}{\sqrt{d}} \boldsymbol{\Omega} \left(\sigma^2 \sum_{i=1}^n \frac{\mathbf{x}^i}{\sqrt{d}} \frac{\mathbf{x}^i}{\sqrt{d}}^\top \right) \boldsymbol{\Omega}^\top \frac{\mathbf{x}}{\sqrt{d}} \\
&= \frac{1}{\sigma^2} \frac{\mathbf{x}^\top}{\sqrt{d}} \boldsymbol{\Omega} \left(\sum_{i=1}^n \frac{\mathbf{x}^i}{\sqrt{d}} \frac{\mathbf{x}^i}{\sqrt{d}}^\top \right) \boldsymbol{\Omega}^\top \frac{\mathbf{x}}{\sqrt{d}}.
\end{aligned} \tag{43}$$

Recall that $\hat{\boldsymbol{\Sigma}} := \frac{1}{n} \sum_{i=1}^n \mathbf{x}^i \mathbf{x}^{i\top}$. Then

$$\begin{aligned}
\sum_{i=1}^n \frac{\mathbf{x}^i}{\sqrt{d}} \frac{\mathbf{x}^i}{\sqrt{d}}^\top &= \frac{1}{d} \sum_{i=1}^n \mathbf{x}^i \mathbf{x}^{i\top} = \frac{n}{d} \hat{\boldsymbol{\Sigma}} = \frac{1}{\alpha} \hat{\boldsymbol{\Sigma}}, \\
\boldsymbol{\Omega} &= \sigma^2 \alpha (\hat{\boldsymbol{\Sigma}} + \hat{R}\mathbf{I})^{-1}.
\end{aligned} \tag{44}$$

Substituting this into equation 43 yields

$$\text{Var}(Z(\mathbf{x}) \mid \mathcal{D}, \mathbf{x}) \tag{45}$$

$$\begin{aligned}
&= \frac{1}{\sigma^2 \alpha} \frac{\mathbf{x}^\top}{\sqrt{d}} [\sigma^2 \alpha (\hat{\boldsymbol{\Sigma}} + \hat{R}\mathbf{I})^{-1}] \hat{\boldsymbol{\Sigma}} [\sigma^2 \alpha (\hat{\boldsymbol{\Sigma}} + \hat{R}\mathbf{I})^{-1}] \frac{\mathbf{x}}{\sqrt{d}} \\
&= \sigma^2 \alpha \frac{\mathbf{x}^\top}{\sqrt{d}} (\hat{\boldsymbol{\Sigma}} + \hat{R}\mathbf{I})^{-1} \hat{\boldsymbol{\Sigma}} (\hat{\boldsymbol{\Sigma}} + \hat{R}\mathbf{I})^{-1} \frac{\mathbf{x}}{\sqrt{d}}.
\end{aligned} \tag{46}$$

Let $\mathbf{x} \sim \mathcal{N}(0, \boldsymbol{\Sigma})$ be independent of \mathcal{D} , and recall $\frac{\mathbf{x}}{\sqrt{d}} = \mathbf{x}/\sqrt{d}$. For any fixed $d \times d$ matrix A ,

$$\mathbb{E}_{\mathbf{x}} \left[\frac{\mathbf{x}^\top}{\sqrt{d}} A \frac{\mathbf{x}}{\sqrt{d}} \right] = \frac{1}{d} \mathbb{E}_{\mathbf{x}} [\mathbf{x}^\top A \mathbf{x}] = \frac{1}{d} \text{Tr}(A\boldsymbol{\Sigma}).$$

Applying this to equation 46 gives

$$\begin{aligned}
&\mathbb{E}_{\mathbf{x}} [\text{Var}(Z(\mathbf{x}) \mid \mathcal{D}, \mathbf{x})] \\
&= \sigma^2 \alpha \frac{1}{d} \text{Tr}((\hat{\boldsymbol{\Sigma}} + \hat{R}\mathbf{I})^{-1} \hat{\boldsymbol{\Sigma}} (\hat{\boldsymbol{\Sigma}} + \hat{R}\mathbf{I})^{-1} \boldsymbol{\Sigma}).
\end{aligned} \tag{47}$$

Since $\mathbb{E}[Z(\mathbf{x}) \mid \mathcal{D}, \mathbf{x}] = 0$, the unconditional variance is

$$\text{Var}(Z(\mathbf{x})) = \mathbb{E}_{\mathcal{D}, \mathbf{x}} [\text{Var}(Z(\mathbf{x}) \mid \mathcal{D}, \mathbf{x})], \tag{48}$$

so taking expectation over \mathcal{D} in equation 47 yields

$$\text{Var}(Z(\mathbf{x})) = \sigma^2 \alpha \mathbb{E}_{\mathcal{D}} \left[\frac{1}{d} \text{Tr}((\hat{\boldsymbol{\Sigma}} + \hat{R}\mathbf{I})^{-1} \hat{\boldsymbol{\Sigma}} (\hat{\boldsymbol{\Sigma}} + \hat{R}\mathbf{I})^{-1} \boldsymbol{\Sigma}) \right]. \tag{49}$$

We now invoke the same deterministic-equivalent machinery. One obtains

$$\frac{1}{d} \text{Tr}((\hat{\boldsymbol{\Sigma}} + \hat{R}\mathbf{I})^{-1} \hat{\boldsymbol{\Sigma}} (\hat{\boldsymbol{\Sigma}} + \hat{R}\mathbf{I})^{-1} \boldsymbol{\Sigma}) \xrightarrow[d, n \rightarrow \infty]{\mathbb{P}} \frac{\alpha m_{\boldsymbol{\Sigma}}^{(2)}(R)}{1 - \alpha m_{\boldsymbol{\Sigma}}^{(2)}(R)}, \tag{50}$$

where

$$m_{\boldsymbol{\Sigma}}^{(2)}(R) = \frac{1}{d} \text{Tr}[\boldsymbol{\Sigma}^2 (\boldsymbol{\Sigma} + R\mathbf{I})^{-2}].$$

Substituting the deterministic equivalent equation 50 into equation 49, we obtain, as $d, n \rightarrow \infty$ with α fixed,

$$\begin{aligned}
\text{Var}(Z(\mathbf{x})) &= \sigma^2 \alpha \frac{1}{d} \text{Tr}((\hat{\boldsymbol{\Sigma}} + \hat{R}\mathbf{I})^{-1} \hat{\boldsymbol{\Sigma}} (\hat{\boldsymbol{\Sigma}} + \hat{R}\mathbf{I})^{-1} \boldsymbol{\Sigma}) \\
&= \sigma^2 \frac{\alpha m_{\boldsymbol{\Sigma}}^{(2)}(R)}{1 - \alpha m_{\boldsymbol{\Sigma}}^{(2)}(R)}.
\end{aligned} \tag{51}$$

Here we can ignore this contribution as long as

$$\sigma^2 \ll \frac{1 - \alpha m_{\boldsymbol{\Sigma}}^{(2)}(R)}{\alpha m_{\boldsymbol{\Sigma}}^{(2)}(R)} = \sigma_c(\alpha, R)^2 \tag{52}$$

C PROOF OF RESULT 2

Result 10. For $T \gg s(\mathbf{x})^2$ the expectation value of the error can be organized as a perturbative series as follows

$$\begin{aligned}\delta &= \mathbb{E}_{\mathbf{x}} \left[\Delta_T(\mathbf{x})^2 + s^2(\mathbf{x}) \right. \\ &\quad \left. + \sum_{l=1}^3 (-1)^l \frac{C_l(\mathbf{x})}{t(\mathbf{x})^l} \prod_{i=1}^l \left(1 - \frac{i}{k}\right) + \mathcal{O}\left(t(\mathbf{x})^{-4}\right) \right]\end{aligned}\quad (53)$$

Where we have defined $t(\mathbf{x}) = \frac{T}{2s(\mathbf{x})^2}$ and

$$C_l(\mathbf{x}) = 2\Delta_T(\mathbf{x})\Delta_R(\mathbf{x}) + s^2(\mathbf{x}) + (l-1)\Delta_R(\mathbf{x})^2 \quad (54)$$

$$\Delta_T(\mathbf{x}) := m(\mathbf{x}) - \mu_T(\mathbf{x}), \quad \Delta_R(\mathbf{x}) := m(\mathbf{x}) - \mu_R(\mathbf{x}). \quad (55)$$

All other quantities are as in Result 1.

Proof-sketch. Consider a random variable x and we are interested in concentration properties of the function $f(x) = \log x$. Here we will discuss a controlled approximation technique to evaluate the expectation value of f . Simplest approach is to Taylor expand f around the expectation value of x denoted by \bar{x}

$$\begin{aligned}f(x) &= \log \bar{x} + \frac{1}{\bar{x}}(x - \bar{x}) - \frac{1}{2\bar{x}^2}(x - \bar{x})^2 \\ &\quad + \frac{1}{3\bar{x}^3}(x - \bar{x})^3 + \mathcal{O}\left(\frac{(x - \bar{x})^4}{\bar{x}^4}\right)\end{aligned}\quad (56)$$

Taking expectation value of both sides of the equation above we get the following expression

$$\begin{aligned}\mathbb{E}(\log x) &= \log \mathbb{E}(x) - \frac{\mathbb{E}(x^2) - \mathbb{E}(x)^2}{2\mathbb{E}(x)^2} \\ &\quad + \frac{\mathbb{E}(x^3) - 3\mathbb{E}(x^2)\mathbb{E}(x) + 2\mathbb{E}(x)^3}{3\mathbb{E}(x)^3} + \mathcal{O}\left(\frac{\mathbb{E}((x - \mathbb{E}(x))^4)}{\mathbb{E}(x)^4}\right)\end{aligned}\quad (57)$$

This approximation scheme is only useful when higher order corrections are relatively small. Next we use this to derive the result stated in the Result above.

It will be convenient to define partition function density given by

$$z(\mathbf{J}, \mathbf{p}) = \frac{1}{k} \sum_{i=1}^k e^{-\frac{1}{T} E_{\mathbf{w}_R}(p_i) - J_i E_{\mathbf{w}_T}(p_i)}, \quad E_{\mathbf{w}}(p) = (p - \mathbf{w} \cdot \frac{\mathbf{x}}{\sqrt{d}})^2 \quad (58)$$

The expectation value of $z(\mathbf{J}, \mathbf{p})$ when p_i is sampled from the following distribution

$$p_i \sim \mathcal{N}(m, \Sigma = s^2), \quad i = 1, 2, \dots, k \quad (59)$$

gives disorder averaged, over k samples, partition function, with an additional chemical potential \mathbf{J} , of free particles at temperature T . The error given in (7) can be expressed in terms of this quantity as follows

$$\begin{aligned}\delta &= \mathbb{E}_{\mathbf{p}} \left(\frac{\sum_{i=1}^k E_{\mathbf{w}_T}(p_i) e^{-\frac{1}{T} E_{\mathbf{w}_R}(p_i) - J_i E_{\mathbf{w}_T}(p_i)}}{\sum_{i=1}^k e^{-\frac{1}{T} E_{\mathbf{w}_R}(p_i) - J_i E_{\mathbf{w}_T}(p_i)}} \right) \\ &= -\mathbb{E}_{\mathbf{p}} \sum_i \partial_{J_i} (\log z(\mathbf{J}, \mathbf{p}))|_{\mathbf{J}=0} \\ &\approx -\sum_i \partial_{J_i} \left(\log \mathbb{E}_{\mathbf{p}}(z(\mathbf{J}, \mathbf{p})) - \frac{\mathbb{E}_{\mathbf{p}}(z(\mathbf{J}, \mathbf{p})^2) - \mathbb{E}_{\mathbf{p}}(z(\mathbf{J}, \mathbf{p}))^2}{2\mathbb{E}_{\mathbf{p}}(z(\mathbf{J}, \mathbf{p}))^2} \right. \\ &\quad \left. + \frac{\mathbb{E}_{\mathbf{p}}(z(\mathbf{J}, \mathbf{p})^3) - 3\mathbb{E}_{\mathbf{p}}(z(\mathbf{J}, \mathbf{p})^2)\mathbb{E}_{\mathbf{p}}(z(\mathbf{J}, \mathbf{p})) + 2\mathbb{E}_{\mathbf{p}}(z(\mathbf{J}, \mathbf{p}))^3}{3\mathbb{E}_{\mathbf{p}}(z(\mathbf{J}, \mathbf{p}))^3} \right)|_{\mathbf{J}=0}\end{aligned}\quad (60)$$

To go from the second to the third line we have made an approximation, we will present the domain of validity of the approximation shortly. To this end we compute,

$$\mathbb{E}_{\mathbf{p}}(z(\mathbf{J}, \mathbf{p})) = \frac{1}{k} \sum_{i=1}^k \mathbb{E}_p(e^{-\frac{1}{T} E_{\mathbf{w}_R}(p) - J_i E_{\mathbf{w}_T}(p)}) \quad (61)$$

The required expectation values can be expressed in terms of the following function

$$\begin{aligned}
& h(m_1, m_2, m_3; s_1^2, s_2^2, s_3^2) \\
& \quad \sum_{\substack{1 \leq i \neq j \neq k \leq 3}} \frac{(\frac{1}{2}m_i^2(s_j^2 + s_k^2) - m_i m_j s_k^2)}{\exp\left[-\frac{1}{2\prod_{i=1}^3 s_i^2} \sum_{i=1}^3 \frac{1}{s_i^2}\right]} \\
& = \frac{2 \prod_{i=1}^3 s_i^2 \sum_{i=1}^3 \frac{1}{s_i^2}}{2\pi \sqrt{\prod_{i=1}^3 s_i^2 \sum_{i=1}^3 \frac{1}{s_i^2}}}. \tag{62}
\end{aligned}$$

The moments of $z(\mathbf{J}, \mathbf{p})$ are given by

$$\begin{aligned}
& \mathbb{E}_{\mathbf{p}}[z(\mathbf{J}, \mathbf{p})] \\
& = \frac{1}{k} \sum_{i=1}^k \pi \sqrt{\frac{T}{J_i}} h\left(m, \frac{\mathbf{w}_R \cdot \mathbf{x}}{\sqrt{d}}, \frac{\mathbf{w}_T \cdot \mathbf{x}}{\sqrt{d}}; s^2, \frac{T}{2}, \frac{1}{2J_i}\right), \tag{63}
\end{aligned}$$

$$\begin{aligned}
\mathbb{E}_{\mathbf{p}}[z(\mathbf{J}, \mathbf{p})^2] & = \frac{1}{k^2} \left[\sum_{\substack{i,j=1 \\ i \neq j}}^k \pi \sqrt{\frac{T}{J_i}} h\left(m, \frac{\mathbf{w}_R \cdot \mathbf{x}}{\sqrt{d}}, \frac{\mathbf{w}_T \cdot \mathbf{x}}{\sqrt{d}}; s^2, \frac{T}{2}, \frac{1}{2J_i}\right) \right. \\
& \quad \times \pi \sqrt{\frac{T}{J_j}} h\left(m, \frac{\mathbf{w}_R \cdot \mathbf{x}}{\sqrt{d}}, \frac{\mathbf{w}_T \cdot \mathbf{x}}{\sqrt{d}}; s^2, \frac{T}{2}, \frac{1}{2J_j}\right) \\
& \quad \left. + \sum_{i=1}^k \pi \sqrt{\frac{T}{4J_i}} h\left(m, \frac{\mathbf{w}_R \cdot \mathbf{x}}{\sqrt{d}}, \frac{\mathbf{w}_T \cdot \mathbf{x}}{\sqrt{d}}; s^2, \frac{T}{4}, \frac{1}{4J_i}\right) \right],
\end{aligned}$$

$$\begin{aligned}
\mathbb{E}_{\mathbf{p}}[z(\mathbf{J}, \mathbf{p})^3] & = \frac{1}{k^3} \left[\sum_{1 \leq i < j < \ell \leq k} 6\pi \sqrt{\frac{T}{J_i}} h\left(m, \frac{\mathbf{w}_R \cdot \mathbf{x}}{\sqrt{d}}, \frac{\mathbf{w}_T \cdot \mathbf{x}}{\sqrt{d}}; s^2, \frac{T}{2}, \frac{1}{2J_i}\right) \right. \\
& \quad \times \pi \sqrt{\frac{T}{J_j}} h\left(m, \frac{\mathbf{w}_R \cdot \mathbf{x}}{\sqrt{d}}, \frac{\mathbf{w}_T \cdot \mathbf{x}}{\sqrt{d}}; s^2, \frac{T}{2}, \frac{1}{2J_j}\right) \\
& \quad \times \pi \sqrt{\frac{T}{J_\ell}} h\left(m, \frac{\mathbf{w}_R \cdot \mathbf{x}}{\sqrt{d}}, \frac{\mathbf{w}_T \cdot \mathbf{x}}{\sqrt{d}}; s^2, \frac{T}{2}, \frac{1}{2J_\ell}\right) \\
& \quad + \sum_{\substack{i,j=1 \\ i \neq j}}^k 3\pi \sqrt{\frac{T}{4J_i}} h\left(m, \frac{\mathbf{w}_R \cdot \mathbf{x}}{\sqrt{d}}, \frac{\mathbf{w}_T \cdot \mathbf{x}}{\sqrt{d}}; s^2, \frac{T}{4}, \frac{1}{4J_i}\right) \\
& \quad \times \pi \sqrt{\frac{T}{J_j}} h\left(m, \frac{\mathbf{w}_R \cdot \mathbf{x}}{\sqrt{d}}, \frac{\mathbf{w}_T \cdot \mathbf{x}}{\sqrt{d}}; s^2, \frac{T}{2}, \frac{1}{2J_j}\right) \\
& \quad \left. + \sum_{i=1}^k \pi \sqrt{\frac{T}{9J_i}} h\left(m, \frac{\mathbf{w}_R \cdot \mathbf{x}}{\sqrt{d}}, \frac{\mathbf{w}_T \cdot \mathbf{x}}{\sqrt{d}}; s^2, \frac{T}{6}, \frac{1}{6J_i}\right) \right].
\end{aligned}$$

This leads to the following perturbative expansion in terms of $t = \frac{T}{2s^2}$:

$$\begin{aligned}
\delta(\mathbf{x}) &= (m - \mathbf{w}_T \cdot \frac{\mathbf{x}}{\sqrt{d}})^2 + s^2 \\
&\quad - \frac{1}{t} \left(1 - \frac{1}{k}\right) \left((m - \frac{\mathbf{w}_R \cdot \mathbf{x}}{\sqrt{d}}) \left(2(m - \frac{\mathbf{w}_T \cdot \mathbf{x}}{\sqrt{d}})\right) + s^2 \right) \\
&\quad + \frac{1}{t^2} \left(1 - \frac{1}{k}\right) \left(1 - \frac{2}{k}\right) \\
&\quad \times \left(\left(m - \frac{\mathbf{w}_R \cdot \mathbf{x}}{\sqrt{d}}\right) \left(2 \left(m - \frac{\mathbf{w}_T \cdot \mathbf{x}}{\sqrt{d}}\right) + \left(m - \frac{\mathbf{w}_R \cdot \mathbf{x}}{\sqrt{d}}\right)\right) + s^2 \right) \\
&\quad + O\left(\frac{1}{t^3}\right)
\end{aligned} \tag{64}$$

Repeating this technique to higher order is straight forward but algebraically tedious. Here we quote the result to one higher order

$$\begin{aligned}
\delta(\mathbf{x}) &= (m - \mathbf{w}_T \cdot \frac{\mathbf{x}}{\sqrt{d}})^2 + s^2 \\
&\quad + \sum_{l=1}^3 (-1)^l \left(1 - \frac{1}{k}\right) \left(1 - \frac{2}{k}\right) \dots \left(1 - \frac{l}{k}\right) \frac{1}{t^l} C_l(\mathbf{x}) \\
&\quad + O\left(\frac{1}{t^4}\right) \\
C_l(\mathbf{x}) &= 2 \left(m - \frac{\mathbf{w}_R \cdot \mathbf{x}}{\sqrt{d}}\right) \left(m - \frac{\mathbf{w}_T \cdot \mathbf{x}}{\sqrt{d}}\right) \\
&\quad + s^2(\mathbf{x}) + (l-1) \left(m - \frac{\mathbf{w}_R \cdot \mathbf{x}}{\sqrt{d}}\right)^2
\end{aligned} \tag{65}$$

D PROOF OF RESULT 3

Result 11 (Low- T best-of- k sampling). *When we have access to the exact teacher weight $\mathbf{w}_R = \mathbf{w}_T = \mathbf{w}$, the leading order result for $T \rightarrow 0$ followed by $k \rightarrow \infty$ is given by*

$$\delta(\mathbf{x}) = \frac{\pi}{k^2} s^2(\mathbf{x}) \exp\left(\frac{\Delta_T(\mathbf{x})^2}{s^2(\mathbf{x})}\right) \tag{66}$$

All the quantities are as in Result 1 and Result 2.

Proof-sketch. In $T \rightarrow 0$ limit it is natural to approximate the softmax by the sample with highest reward, i.e.,

$$\begin{aligned}
\delta(\mathbf{x}) &= \mathbb{E}_{y_i \sim \mathcal{N}(m, \Sigma), i=1, \dots, k} \left(\left(y'_k - \mathbf{w}_T \cdot \frac{\mathbf{x}}{\sqrt{d}} \right)^2 : \right. \\
&\quad \left. y'_k = \arg \min_{y \in (y_1, y_2, \dots, y_k)} \left(y - \mathbf{w}_R \cdot \frac{\mathbf{x}}{\sqrt{d}} \right)^2 \right) \\
&\quad \tag{67}
\end{aligned}$$

First note that the distribution of the penalty is a non-central chi-squared distribution with one degree of freedom:

$$-v \equiv \frac{1}{s^2} \left(y - \mathbf{w}_R \cdot \frac{\mathbf{x}}{\sqrt{d}} \right)^2 \sim \chi_1^2(\lambda), \lambda = \frac{(m - \mathbf{w}_R \cdot \frac{\mathbf{x}}{\sqrt{d}})^2}{s^2} \tag{68}$$

We focus on the situation of perfect reward $\mathbf{w}_R = \mathbf{w}_T$ in the high reward regime. In this case,

$$\delta(\mathbf{x}) = s^2 \mathbb{E}(-v_{max}), \quad v_{max} = \max_{-v_i \sim \chi_1^2(\lambda)} (v_1, v_2, \dots, v_k) \tag{69}$$

Since we are looking for the minimum of the chi-squared distributed variables the extreme value statistics is more involved and the final distribution is different compared to the analysis for maximum.

Next we focus on $k \rightarrow \infty$ limit for analytical tractability. Probability distribution function φ and cumulative distribution function F of $v \leq 0$ is given by

$$\begin{aligned}\varphi(v) &= \frac{e^{\frac{v-\lambda}{2}} \cos(\sqrt{\lambda}v)}{\sqrt{2\pi}\sqrt{-v}}, \\ F(v) &= 1 - \frac{1}{2} \left(\operatorname{erf}\left(\frac{\sqrt{-v} - \sqrt{\lambda}}{\sqrt{2}}\right) + \operatorname{erf}\left(\frac{\sqrt{\lambda} + \sqrt{-v}}{\sqrt{2}}\right) \right)\end{aligned}\quad (70)$$

Note that as $k \rightarrow \infty$ the degenerate distribution concentrates near $v_F = 0$. Given that v_F is finite, the extreme distribution could be either of Weibull or Gumbel type. Next we show that it is not Gumbel type. To see this we calculate the auxiliary function for the Gumbel type using

$$a(v) = \frac{1 - F(v)}{F'(v)}, \quad \lim_{v \rightarrow v_F} a'(v) \neq 0 \quad (71)$$

This limit on right ensures it cannot be of Gumbel type. To identify the Weibull distribution

$$\Psi_\alpha(x) = e^{-(x)^\alpha} \quad \text{for } x \leq 0, \quad 1 \quad \text{otherwise} \quad (72)$$

We calculate

$$\alpha = \lim_{v \rightarrow v_F} \frac{(v_F - v)F'(v)}{1 - F(v)} = \frac{1}{2} \quad (73)$$

This ensures the cumulative distribution function of $(v_{max} - d_k)/c_k$ is Ψ_α where

$$\begin{aligned}d_k &= v_F = 0 \\ c_k &= v_F - F^{-1}\left(1 - \frac{1}{k}\right) = \frac{\pi}{2k^2} e^\lambda\end{aligned}\quad (74)$$

The probability density for $-v_{max}/c_k$ is

$$p_{max}(-v_{max}/c_k) = \alpha(-v_{max}/c_k)^{\alpha-1} e^{-(v_{max}/c_k)^\alpha}, \quad v_{max} \leq 0 \quad (75)$$

This gives the following expression for the error in $t \rightarrow 0, k \rightarrow \infty$ limit (taken in this order)

$$\begin{aligned}\delta(\mathbf{x}) &= s^2 c_k \mathbb{E}(-v_{max}/c_k) \\ &= s^2 c_k \Gamma(1 + 1/\alpha) \\ &= \frac{\pi s^2}{k^2} e^{\frac{(m-\mathbf{w} \cdot \frac{\mathbf{x}_d}{\sqrt{d}})^2}{s^2}}\end{aligned}\quad (76)$$

E PROOF OF REMARK 6

Remark 8. *Given access to exact teacher weight, it is beneficial to scale inference-time compute over adding more training samples in the following regime: consider $T \rightarrow 0$ followed by $k \rightarrow \infty$ with*

$$\frac{\gamma^2}{d} \operatorname{Tr}(\mathbf{B}_R \boldsymbol{\Sigma}) \ll \sigma^2, \quad R \ll \sigma^2 \quad (77)$$

That is within this domain,

$$\frac{\partial \log \delta}{\partial \log k} = -2, \quad \frac{\partial \log \delta}{\partial \log n} = -\frac{\alpha \partial_\alpha(\mathbf{u}^\top \boldsymbol{\Sigma} \mathbf{u})}{\sigma^2 d - 2\mathbf{u}^\top \boldsymbol{\Sigma} \mathbf{u}} \quad (78)$$

and hence

$$\left| \frac{\partial \log \delta}{\partial \log k} \right| \gg \left| \frac{\partial \log \delta}{\partial \log n} \right| \quad (79)$$

Proof-sketch. Our goal is to put upper bound on the magnitude of the derivative w.r.t. n . We proceed systematically by working in the eigen basis of sample variance. By the spectral Theorem for real symmetric matrices, there exists an orthogonal matrix $Q \in O(d)$ and a diagonal $\Lambda = \operatorname{diag}(\lambda_1, \dots, \lambda_d)$ with $\lambda_i \geq 0$ such that

$$\boldsymbol{\Sigma} = Q \Lambda Q^\top, \quad \mathbf{B}_R = Q \operatorname{diag}\left(\frac{R}{\lambda_i + R}\right) Q^\top.$$

This immediately gives following inequalities

$$m_{\Sigma}(R) = \frac{1}{d} \text{Tr}[\Sigma(\Sigma + R\mathbf{I})^{-1}] = \frac{1}{d} \sum_{i=1}^d \frac{\lambda_i}{\lambda_i + R} < 1 \quad (80)$$

$$m'_{\Sigma}(R) = -\frac{1}{d} \text{Tr}[\Sigma(\Sigma + R\mathbf{I})^{-2}] = -\frac{1}{d} \sum_{i=1}^d \frac{\lambda_i}{(\lambda_i + R)^2} \leq 0 \quad (81)$$

We are interested in putting upper bound on the following quantity

$$\begin{aligned} \alpha \partial_{\alpha}(\mathbf{u}^{\top} \Sigma \mathbf{u}) &= \alpha F'(R) \frac{dR}{d\alpha}, \\ F(R) &= \mathbf{u}^{\top} \Sigma \mathbf{u} = \sum_{i=1}^d \frac{R^2 \lambda_i}{(\lambda_i + R)^2} \tilde{w}_i^2, \quad \tilde{\mathbf{w}} = Q^{\top} \mathbf{w} \end{aligned} \quad (82)$$

We will first derive an upper bound on $F'(R)$ and an upper bound on $\frac{dR}{d\alpha}$. To this goal we proceed by noting that $\max_{\lambda \geq 0} \frac{\lambda^2}{(\lambda + R)^3} = \frac{4}{27} \frac{1}{R}$ (attained at $\lambda = 2R$) and we have

$$F'(R) = \sum_{i=1}^d \frac{2R \lambda_i^2}{(\lambda_i + R)^3} \tilde{w}_i^2 \leq 2R \cdot \frac{4}{27} \frac{1}{R} \|\mathbf{w}\|^2 = \frac{8}{27} d.$$

Next we focus on the deterministic equivalents equation

$$\hat{R} = R(1 - \alpha m_{\Sigma}(R)), \quad \hat{R} = \frac{\sigma^2 \alpha}{\gamma^2}.$$

Differentiate both sides w.r.t. α :

$$\left((1 - \alpha m_{\Sigma}) - \alpha R m'_{\Sigma} \right) R' = \frac{\sigma^2}{\gamma^2} + R m_{\Sigma}(R).$$

Using the inequalities in equation (80)

$$R' \leq \frac{\frac{\sigma^2}{\gamma^2} + R m_{\Sigma}(R)}{\hat{R}/R} \leq \frac{\frac{\sigma^2}{\gamma^2} + R}{\hat{R}/R} = \frac{\sigma^2}{\gamma^2} \frac{R}{\hat{R}} + \frac{R^2}{\hat{R}}.$$

This gives us the desired upper bound

$$\alpha \partial_{\alpha}(\mathbf{u}^{\top} \Sigma \mathbf{u}) = \alpha F'(R) \frac{dR}{d\alpha} \leq \frac{8}{27} d \left(R + \frac{\gamma^2 R^2}{\sigma^2} \right).$$

Finally we aim for establishing a lower bound on $\sigma^2 d - 2 \mathbf{u}^{\top} \Sigma \mathbf{u}$. This is achieved by the following observation

$$\frac{R^2 \lambda}{(\lambda + R)^2} \leq \frac{R^2 (\lambda + R)}{(\lambda + R)^2} = \frac{R^2}{\lambda + R} \leq R,$$

Hence

$$\mathbf{u}^{\top} \Sigma \mathbf{u} = \sum_{i=1}^d \frac{R^2 \lambda_i}{(\lambda_i + R)^2} \tilde{w}_i^2 \leq R \sum_{i=1}^d \tilde{w}_i^2 = R \|\mathbf{w}\|^2 = R d.$$

Therefore

$$\sigma^2 d - 2 \mathbf{u}^{\top} \Sigma \mathbf{u} \geq d(\sigma^2 - 2R).$$

Putting both the results together, when $R/\sigma^2 \ll 1$ we get

$$\left| \frac{\partial \log \delta}{\partial \log n} \right| \leq \frac{\frac{8}{27} d (R + \gamma^2 R^2 / \sigma^2)}{d(\sigma^2 - 2R)} = \frac{8}{27} \cdot \frac{R}{\sigma^2} \cdot \frac{1 + \gamma^2 R / \sigma^2}{1 - 2R / \sigma^2} \ll 1$$

F GOING BEYOND INDEPENDENT INFERENCE TIME SAMPLING: SELF-CONSISTENCY AND BEAM SEARCH

In this appendix we briefly sketch two speculative extensions of the inference-time sampling-and-selection framework studied in the main text. Both ideas introduce dependence between candidates, going beyond the i.i.d. sampling assumption that enables the clean proportional-limit analysis in this paper. While we do not pursue these directions here, they appear promising and may admit tractable approximations closely related to the calculations already developed.

F.1 SELF-CONSISTENCY

A common heuristic in LLM decoding is to prefer answers that are not only high-reward individually, but also supported by other sampled candidates. This idea is often referred to as self-consistency: candidates that agree with many others are treated as more reliable. We can model this by augmenting the selection score with a consensus kernel:

$$s_i = \sum_{j \neq i} K_\tau(y_i, y_j), \quad K_\tau(y, y') = \exp\left(-\frac{(y - y')^2}{\tau}\right),$$

and scoring each candidate with

$$\underbrace{r(y_i, \mathbf{x})}_{\text{alignment to reward}} + \beta \underbrace{\log s_i}_{\text{alignment to consensus}},$$

for some $\beta \geq 0$. The softmax then uses $\exp([r_R(y_i, \mathbf{x}) + \beta \log s_i]/T)$. For the purpose of analytical calculations it is reasonable to approximate $s_i \rightarrow \mathbb{E}[s_i | y_i]$ in this expression. This in effect rescales T and shifts \mathbf{w}_R . The theoretical analysis can be performed following similar steps as in the paper.

F.2 BEAM SEARCH

Another practically important decoding primitive is beam search, which introduces a structured pruning step before selection. We model a simplified, one-step abstraction of this mechanism as follows. Fix a search budget K (total proposals explored by the decoder) and a beam width $B \in \{1, \dots, K\}$ (candidates kept after pruning). A beam search operator $\mathcal{B}_{K,B}$ keeps the B proposals:

$$\begin{aligned} \{Y_{(1)}, \dots, Y_{(B)}\} &= \mathcal{B}_{K,B}(\{Y_i\}_{i=1}^K) \\ &= \arg \text{top-}B \{-|Y_i - m|\}_{i=1}^K. \end{aligned} \tag{83}$$

These B kept candidates are then passed to our reward-weighted selector (softmax over $r(y, \mathbf{x})$ at temperature T).

The marginal distribution of a kept value under $\mathcal{B}_{K,B}$ is well-approximated by (we take correlations into account later):

$$q_{\text{beam}}(y | \mathbf{x}, \mathcal{D}) \propto \mathcal{N}(y | m, s^2) \mathbf{1}\{|y - m| \leq t_B\},$$

where the truncation threshold t_B is chosen so that the expected keep rate matches B/K :

$$\Pr(|Y - m| \leq t_B) = \frac{B}{K}$$

Under symmetric truncation, the mean remains m and the variance s^2 contracts to s_{beam}^2 .

Even if Y_1, \dots, Y_K are i.i.d., the kept vector $(Y_{(1)}, \dots, Y_{(B)})$ is not independent (order-statistic coupling). A standard correction is to replace k by an effective size k_{eff} such that $\text{Var}(\bar{g}_B) = \text{Var}(g(Y_{(i)})) / k_{\text{eff}}$, $\bar{g}_B = \frac{1}{B} \sum_{i=1}^B g(Y_{(i)})$. Simplest case would correspond to choosing $g(x) = x$.

In summary, we expect that the replacements $s^2 \rightarrow s_{\text{beam}}^2$, $k \rightarrow k_{\text{eff}}$ in our formula would capture the effect of beam search.

G EXPERIMENTAL DETAILS

G.1 BAYESIAN LINEAR REGRESSION BASED MODEL

In this Appendix we present additional numerical results for a broader domain of parameters compared to the main text for Bayesian linear regression based model. We see that the patterns explained in the main body of the paper is realized in a broad domain of parameters.

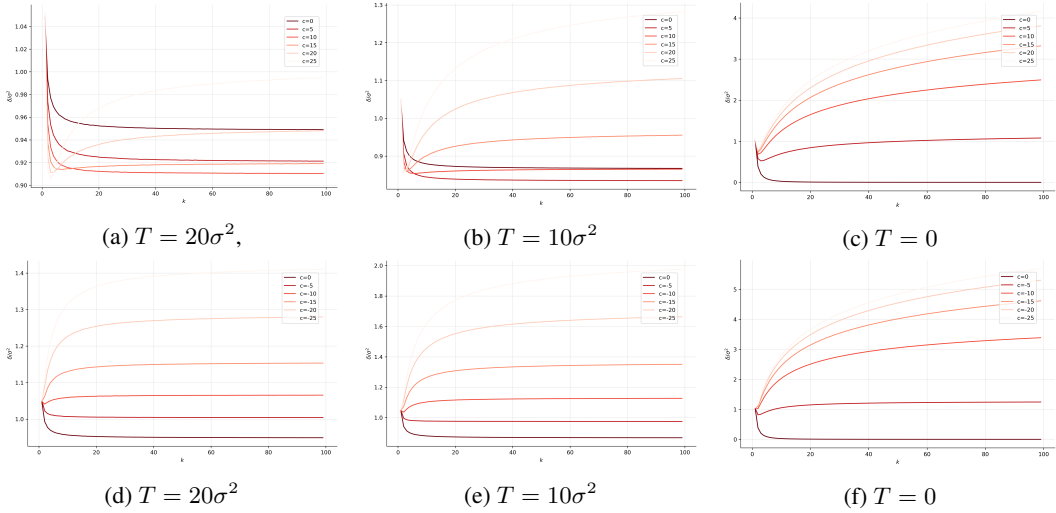


Figure 13: In the plot we have chosen $S = 1, \sigma = 10^{-4}, \gamma = 10^{-3}, n = 10^4, d = 10^1$ and sampled teacher weight $\mathbf{w}_T \sim \mathcal{N}(0, 2^2 \mathbf{I})$. We have parameterized the reward weight as follows: $\mathbf{w}_R = (1 + cR/(R + S^2))\mathbf{w}_T$. The plot shows asymmetry between $c > 0, c < 0$ regions as explained in the main text.

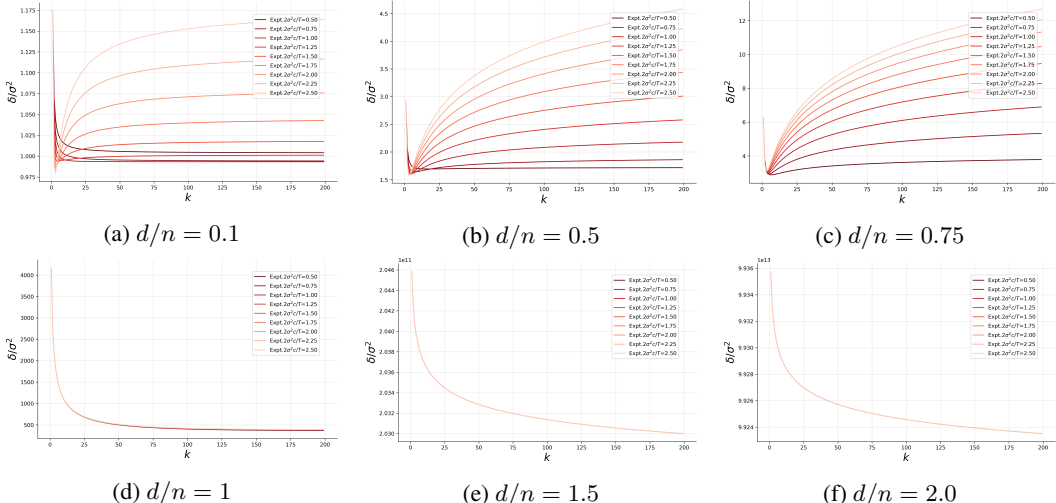


Figure 14: In the plot we have chosen $S = 1, \sigma = 10^{-4}, \gamma = 10^1, n = 10^2, T = 20\sigma^2$ and sampled teacher weight $\mathbf{w}_T \sim \mathcal{N}(0, 2^2 \mathbf{I})$. We have parameterized the reward weight as follows: $\mathbf{w}_R = (1 + cR/(R + S^2))\mathbf{w}_T$. We see that for $d \geq n$ generalization error shows different pattern compared to $d < n$. For $d < n$ we see features that are discussed in the main text. We note that as d/n increases δ at fixed k generally increases. Nevertheless, even for $d \geq n$, an increase in k decreases δ for a wide range of \mathbf{w}_R .

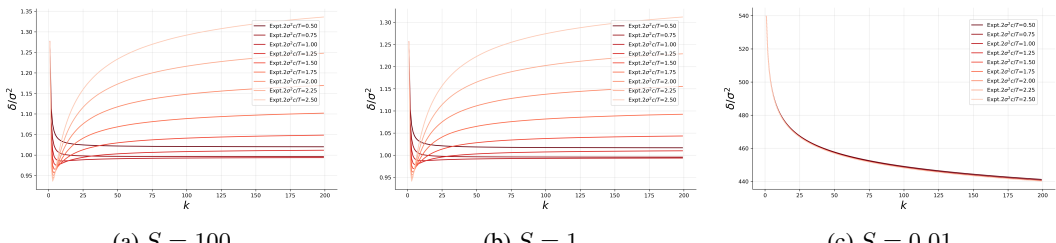


Figure 16: In the plot we have chosen $T = 20\sigma^2, \sigma = 10^{-4}, \gamma = 10^{-2}, n = 10^2, d = 10^1$ and sampled teacher weight $\mathbf{w}_T \sim \mathcal{N}(0, 2^2 \mathbf{I})$. We have parameterized the reward weight as follows: $\mathbf{w}_R = (1 + cR/(R + S^2))\mathbf{w}_T$. The plot shows as S is lowered beyond a critical value we see a sharp change of features.

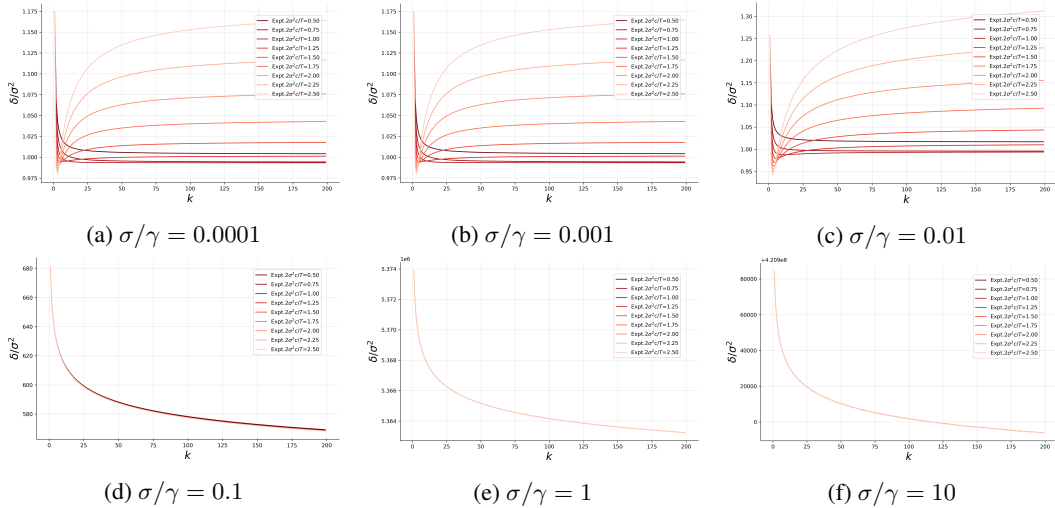


Figure 15: In the plot we have chosen $S = 1, \sigma = 10^{-4}, n = 10^2, d = 10^1, T = 20\sigma^2$ and sampled teacher weight $\mathbf{w}_T \sim \mathcal{N}(0, 2^2 \mathbf{I})$. We have parameterized the reward weight as follows: $\mathbf{w}_R = (1 + cR/(R + S^2))\mathbf{w}_T$. We see that for large σ/γ generalization error shows different pattern compared to small σ/γ . Plots show similarity with the plot of δ vs d/n - in the language of deterministic equivalence both of these are related to the similar change of the un-renormalized ridge.

G.2 LARGE LANGUAGE MODEL

Here we present experimental details for LLM based evaluations presented in the main text along with additional results.

G.2.1 TASK, PROMPTING, AND GENERATION PROTOCOL

We evaluate inference-time scaling on GSM8K validation dataset using the lm-evaluation-harness task `gsm8k_cot_self_consistency`. Our prompt format is chain-of-thought few-shot prompting with 8 CoT exemplars (8-shot CoT) For each test question, the base model is asked to produce a full reasoning trace followed by a final answer in the format “The answer is {number}”. We sample stochastically at generation temperature 0.2. and extract the final numeric answer using a regular expression matching “The answer is (number)”. We also log all reasoning steps to enable Judge-LLM-based selection.

G.2.2 BASE MODELS AND JUDGE MODELS

Base LLMs. We run inference experiments with a diverse set of base large language models: Qwen3-8B, Llama-3-8B-Instruct, Mistral-7B-Instruct-v0.3, deepseek-math-7b-rl, gemma-3-4b-it, and DeepSeek-R1-Distill-Qwen-1.5B. Inference is executed via the `vLLM` backend through `lm_eval` with model-specific `--model_args`, e.g. `tensor/data-parallel` settings.

Judge LLMs. We score each sampled CoT using two types of judge models: process reward model Qwen2.5-Math-PRM-7B and casual LLM Mistral-7B-Instruct-v0.3. For the causal judge, we prompt the judge to output a scalar score in $[0, 10]$. We use a short/weak prompt and a detailed/strong prompt. Examples of each of these prompts are given below. For the PRM, we convert the sampled reasoning into a chat-formatted transcript and insert a step separator token `<extra_0>` after each reasoning step; the PRM score is computed from the model’s per-token probability that each separator is classified as “positive” and then scaled to $[0, 10]$. For judges we use deterministic sampling. PRM based judge is known to be much stronger judge compared to

the causal model based judge. Our experimental results reflect this - for instance Llama model's accuracy increased from 77% to 87% under PRM judge, whereas under causal judge it went up only by 1%.

Model Response Example

Weak prompt: Score 0-10:

[Q] Janet's ducks lay 16 eggs per day. She eats three for breakfast every morning and bakes muffins for her friends every day with four. She sells the remainder at the farmers' market daily for \$ 2 per fresh duck egg. How much in dollars does she make every day at the farmers' market?

[A] Janet's ducks lay 16 eggs per day. She eats 3 and bakes 4, so she has $16 - 3 - 4 = 9$ eggs left. She sells them for 2 dollars each, so she makes $9 \times 2 = 20$ dollars. The answer is 18.

[Final] 18

[Score]:

Judge's response: [0]

Model Response Example

Strong prompt: Score the answer of the student based on its logical consistency of reasoning and accuracy of the final answer. The output should be a number between 0 to 10.

[question] Janet's ducks lay 16 eggs per day. She eats three for breakfast every morning and bakes muffins for her friends every day with four. She sells the remainder at the farmers' market daily for \$ 2 per fresh duck egg. How much in dollars does she make every day at the farmers' market?

[reasoning of the student] Janet's ducks lay 16 eggs per day. She eats 3 and bakes 4, so she has $16 - 3 - 4 = 9$ eggs left. She sells them for 2 dollars each, so she makes $9 \times 2 = 20$ dollars. The answer is 18.

[final answer of the student] 18

[Score]:

Judge's response: [5]

G.2.3 ADDITIONAL RESULTS

In this section we present some more empirical results. For the causal judge we use the strong prompt and for PRM we process the response into multiple steps - we break on sentences that contains an equal sign.

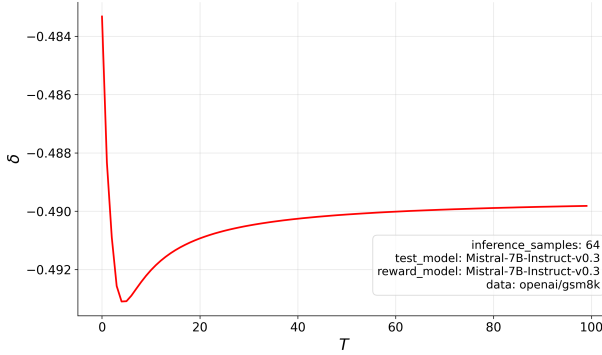


Figure 17: Mistral-7B-Instruct-v0.3 as the base model

In the theoretical model we have seen existence of an optimal temperature for the rewarding process. Graphs above present more experimental evidence in support of it.

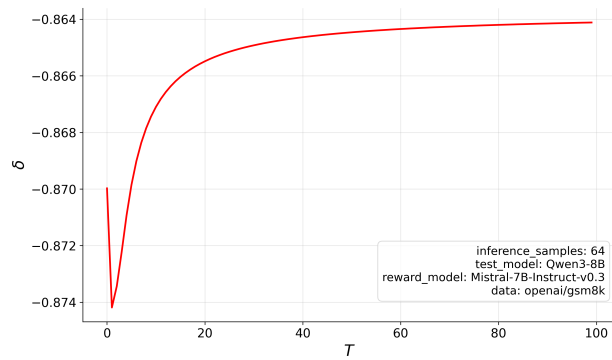


Figure 18: Qwen3-8B as the base model

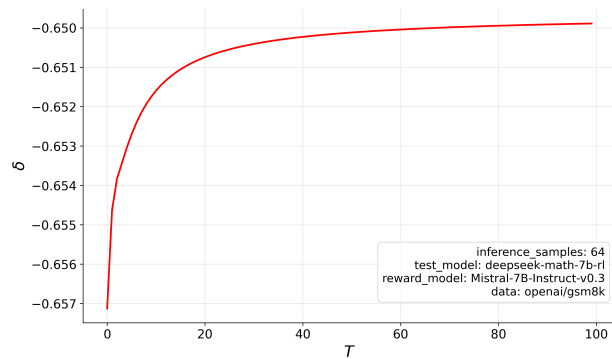


Figure 19: deepseek-math-7b-rl as the base model

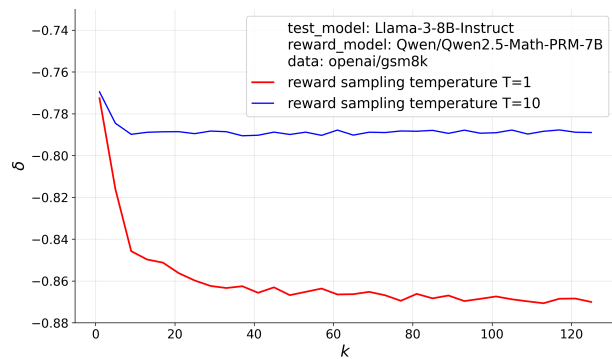


Figure 20: Llama-3-8B-Instruct as base model

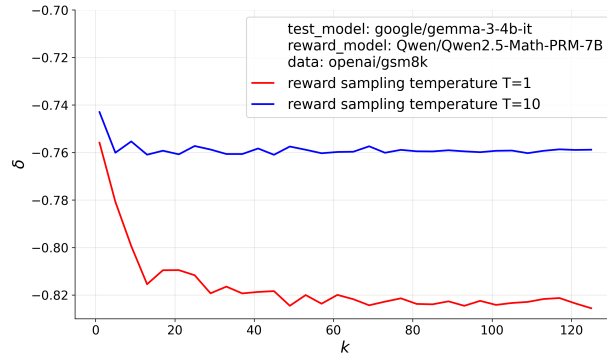


Figure 21: gemma-3-4b-it as base model

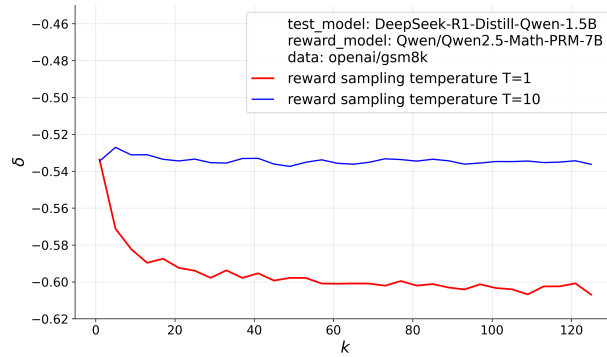


Figure 22: DeepSeek-R1-Distill-Qwen-1.5B as base model

These graphs show that for PRM based judge error keeps on decreasing with increase in number of inference time samples almost monotonically at small temperature.

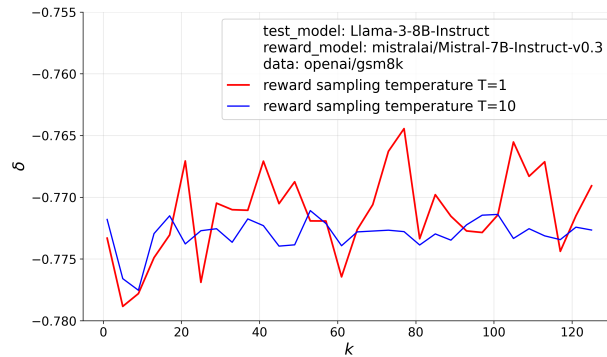


Figure 23: Llama-3-8B-Instruct as base model

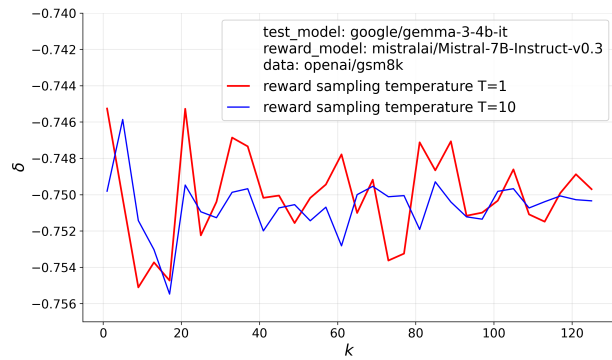


Figure 24: gemma-3-4b-it as base model

These graphs show that for causal LM based judge there exists an optimal value of the inference time samples. This phenomena is theoretically analyzed in the main text of the paper.